R1575

MINERALS RESEARCH

Minerals Research
Progress Report No. 2

July 1973

Department of Chemical and Metallurgical Engineering

Mackay School of Mines

University of Nevada

Reno, Nevada

1.a

TABLE OF CONTENTS

	Page
DISSOLUTION OF ASBESTOS MINERALS IN NEUTRAL SALT SOLUTIONS by M. Allen	1
SPECIAL STUDIES IN ELECTRO-OXIDATION OF CINNABAR by S. Rudy and J. L. Hendrix.	9
ANALYSIS OF ASBESTOS MINERALS USING A VAN DE GRAAF GENERATOR by D. D. Sharma.	24
ADSORPTION OF CARBOXYLIC GROUPS ON Fe_2O_3 by S. Akhtar and S. K. Khanna.	33
THE CORRELATION BETWEEN Ni and Mg DISSOLUTION FROM CHRYSOTILE by M. Allen	37
MIGRATION OF ASBESTOS FIBERS IN THE LYMPHATIC SYSTEM OF MICE by J. E. McGuire and R. E. Thomas	40
CARCINOGENESIS OF ASBESTOS FIBERS AS RELATED TO SURFACE CHEMISTRY by R. E. Thomas.	43

MINERALS RESEARCH

The Department of Chemical and Metallurgical Engineering at the University of Nevada, Reno, is currently engaged in research programs involving (1) the surface chemistry of natural minerals, (2) mineral separation methods, (3) extraction of metals from minerals, and (4) means to reduce atmospheric and water pollution resulting from mineral processing operations.

This progress report is the second of a series that we have issued. The reports are prepared as suitable material is developed. The material in this and subsequent progress reports represents, of course, preliminary results and it should not be quoted without our permission. Criticism and suggestions about the reports and material contained in them will be welcome.

We gratefully acknowledge the financial support of the United States Department of Health, Education and Welfare (grant 2 R01 OH 0332), and the U. S. Bureau of Mines (grants GO-111058 and GO-110303). In addition we gratefully acknowledge the support given us by the Nevada Mining Analytical Laboratory, University of Nevada, Reno.

Ross W Smith

Ross W. Smith
Professor and Chairman
Department of Chemical and
Metallurgical Engineering

Dissolution of Asbestos Minerals in Neutral Salt Solutions*

by: Merrill Allen

Previous work

Kinetic studies have established that the initial dissolution rate of asbestos minerals in water is controlled by the diffusion of products and reactants through the stagnant film at the mineral-solution interface. (1), (2). As dissolution in water continues, the rate becomes controlled by the diffusion of products and reactants through the leached silica shell surrounding the mineral core.(3) The breakdown of the fibers in water is accompanied by an increase in pH, probably caused by the release of OH groups from within the minerals. This pH rise is more rapid for chrysotile suspensions than for either amosite or crocidolite suspensions. (4)

Dissolution of the fibers in acid has been studied by several workers. (5), (6), (7), (8), (9), (10). Rates of cation migration from fibers to solution are much greater in acid than in water at pH 7. In basic solutions silica is readily extracted from the fibers but cations which form insoluble hydroxides remain fixed. (5)

The release of some transition metals (Ni, Cr, Mn) from asbestos fibers in bovine serum has been studied. (11) These metals influence the metabolism of benzpyrene, a known carcinogen, and thus may indirectly link asbestos minerals to lung cancer.(12)

Purpose

The aim of this investigation is to characterize the dissolution of asbestos fibers in a manner related to their dissolution in vivo. By examining the discharge of fiber constituents, such as SiO_2 and the cationic components, in buffered, neutral, aqueous solutions, one may draw reasonable conclusions about fiber dissolution in vivo.

Procedure

Commercial amosite, crocidolite, and chrysotile were used in the study. The three minerals were separately ground in an alundum pebble mill and the -200 mesh fraction used for the dissolution studies.

For each study a one half gram sample of each mineral was weighed and transferred to separate polypropylene centrifuge tubes. Forty ml of leach solution were added to each with a buret and a half inch teflon covered magnet inserted into each tube. The tubes were clamped upright, covered and then stirred using an electrically operated magnetic spin bar driver. The stirring was stopped by an electric timer after one hour. The tubes and contents, including magnetic spinbars, were then centrifuged for five minutes and the clear solution decanted into a # 42 Whatman filter paper in a glass funnel. The filtered solution was received and stored in 40 ml glass centrifuge tubes. Five ml aliquots for silica determinations were withdrawn immediately after filtering and stored in polypropylene beakers. Care was taken not to disturb the mineral and magnet at the bottom of the tube during decanting but occasionally a small amount of mineral, particularly amosite, could be found on the filter paper.

* This research is supported by Dept. of Health, Education and Welfare Grant EC00381.

After the solution was decanted another forty ml volume was added and the stirring, centrifuging, and filtering repeated. This procedure was carried out three times in succession. After the addition of the fourth forty ml volume the solution was stirred for one half hour and allowed to stand overnight. The next morning the solution was stirred again for one half hour, then centrifuged and filtered as in the previous three extractions. The total elapsed time of the third extraction was 18 hours.

Solutions of the following salts were used; KCl, NaCl, KAc, NaAc, NH_4Cl and NH_4Ac. Normal solutions of the first five salts were made by dissolving one mole of a particular salt in water, adjusting the pH to 7 with an appropriate acid or base and then diluting the mixture to one liter. A 1N NH_4Ac solution was prepared by adding 57 ml of glacial acetic acid to about 400 ml of water, adjusting the pH to 7 with concentrated NH_4OH, cooling the solution to room temperature, then diluting it to one liter. Dilutions to 0.1N and 0.01N NH_4Ac were made from the 1N NH_4Ac.

Analyses for silica and the cations were carried out as described in a previous report. (13)

Results

Attention will be focused on Mg and SiO_2 extraction as indexes to fiber dissolution since these two constituents are present in large amounts in all three minerals and are extractable within the pH range of the mineral suspensions. (7-10). Figures 1 and 2 show the extent of dissolution of the three asbestos minerals. after four extractions in the various salt solutions. It is obvious that fiber dissolution increases from amosite to crocidolite to chrysotile in this particular study. The data presented in figures 1 and 2 is arranged to show that fiber dissolution increases with specific surface area.

In a qualitative way, the breakdown of chrysotile can be correlated with the buffer strength of the leach solutions; dissolution being greatest where buffering provided by the salt is the greatest and least where buffering is absent (see Figs. 1 & 2). In the case of amosite and crocidolite it appears that there are no generalizations to be made about buffer strength and dissolution.

Figures 3, 4, and 5 are bar charts showing the amounts of Mg and SiO_2 removed from the minerals during four successive extractions. The length of each vertical line segment is proportional to the amount of a particular constituent removed during an extraction. Magnesium and silica are each discharged from the minerals in different manners. In regard to magnesium removal, in most instances more magnesium is taken into solution during the first extraction than in the three succeeding ones. In terms of elapsed time more magnesium is taken into solution during the first hour than in the last twenty hours. Silica removal from the minerals proceeds more uniformly during the course of the three extractions than does magnesium removal. In most of the salt solutions used on amosite and crpeidolite, the last extraction (18 hours) removed as much silica as the first three (3 hours).

If parallels can be drawn between the breakdown of minerals during these studies and that occurring in vivo, one may conclude that much of the extractable magnesium will be removed quickly. Silica dissolution, while slower than that of magnesium at the outset, will likely proceed at a fairly constant rate. From studies conducted in a similar manner to those presented here but carried out in acidic NH_4Ac solutions, projections have been made from emperical relationships found to exist between fiber

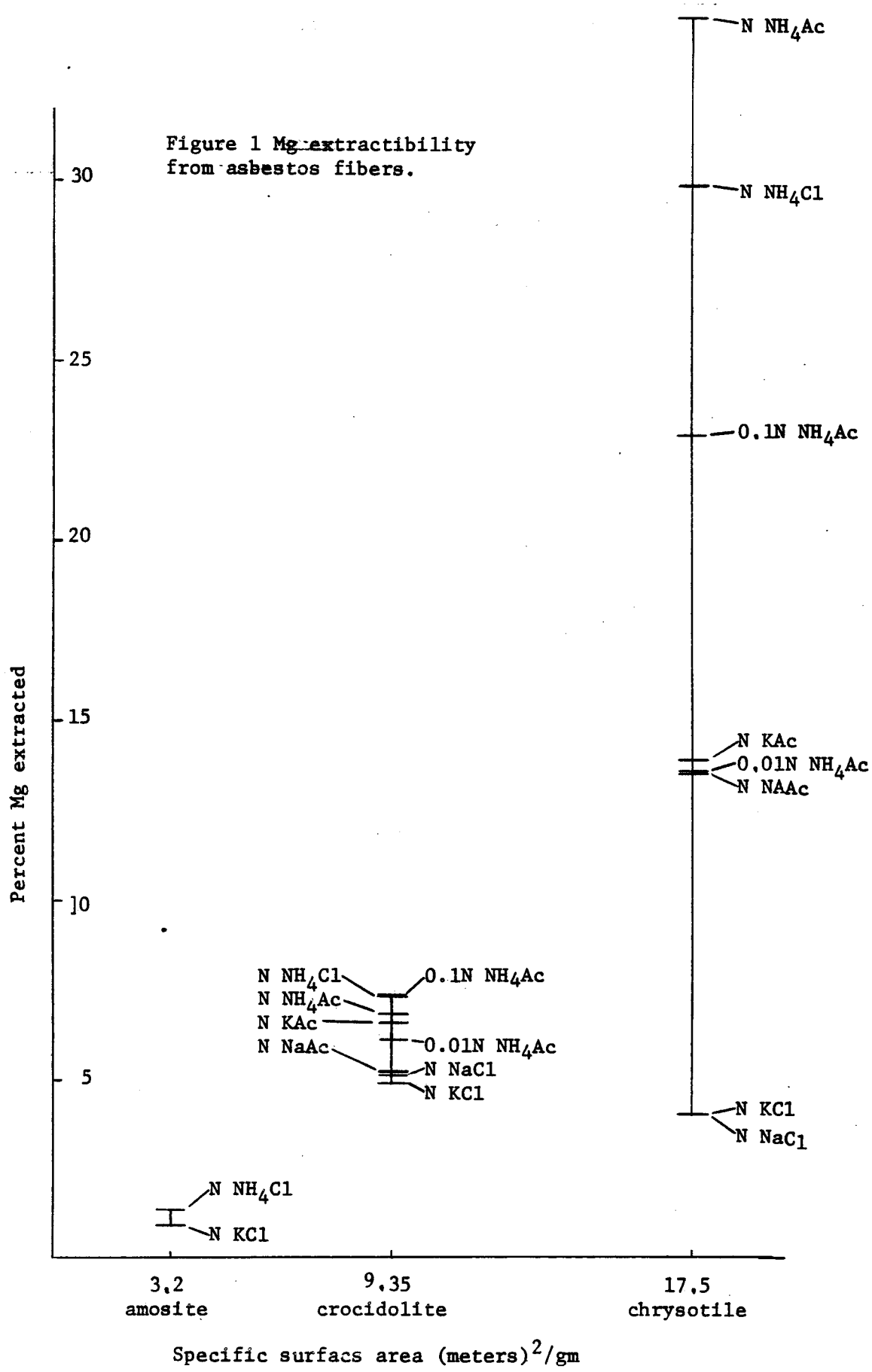
Figure 1 Mg extractibility from asbestos fibers.
Percent Mg extracted
30
25
20
15
10
5
N NH4Ac
N NH4Cl
0.1N NH4Ac
N KAc
0.01N NH4Ac
N NAAc
N KCl
N NaCl
N NH4Cl
N NH4Ac
N KAc
N NaAc
0.1N NH4Ac
0.01N NH4Ac
N NaCl
N KCl
N NH4Cl
N KCl
3.2
amosite
9.35
crocidolite
17.5
chrysotile
Specific surfacs area (meters)2/gm

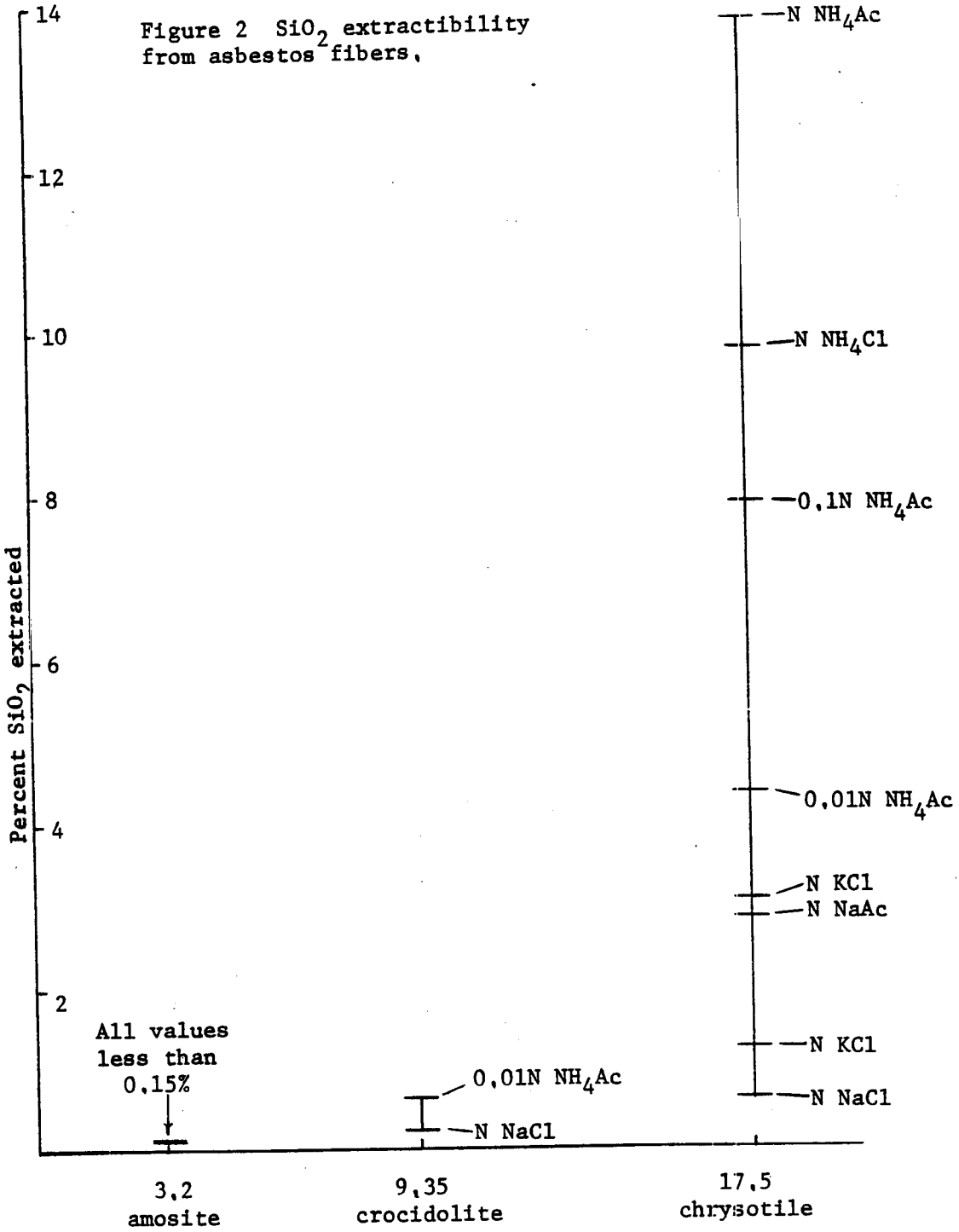

Figure 2 SiO_2 extractibility from asbestos fibers.

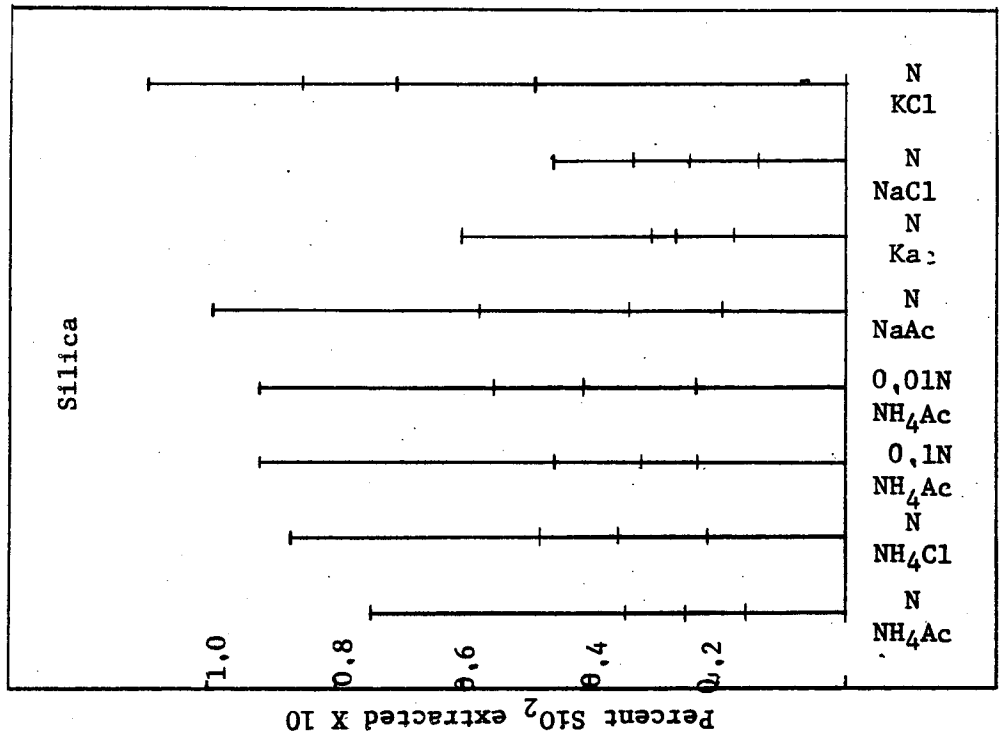

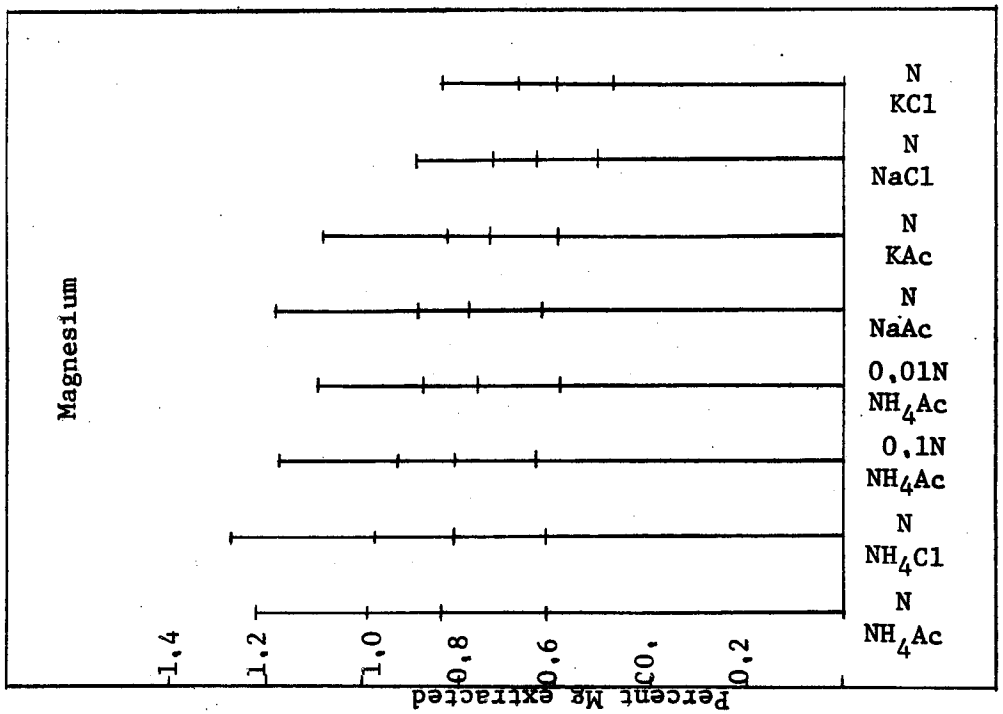

Figure 3. Magnesium and silica removed from amosite using four successive extractions.

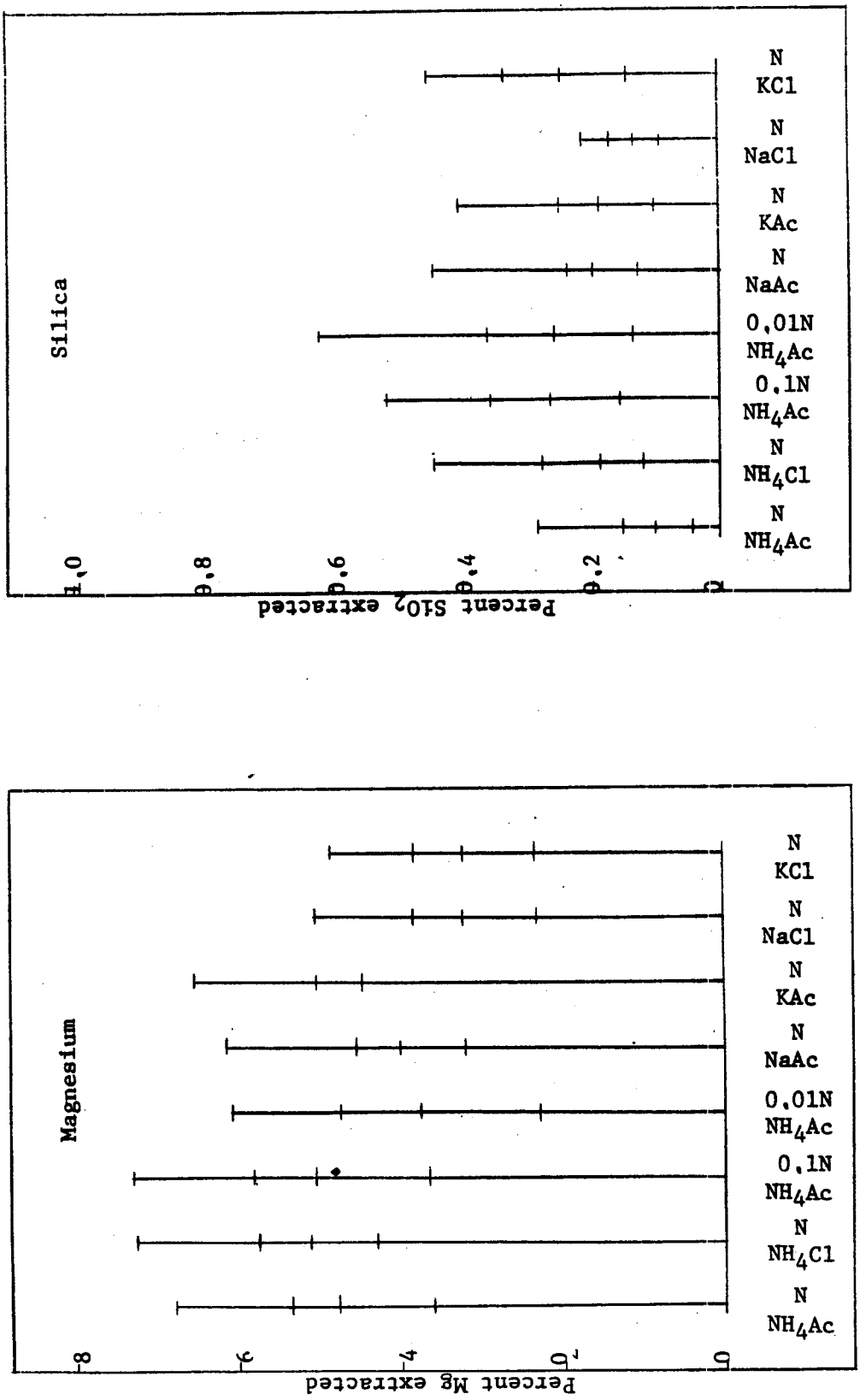

Figure 4. Magnesium and silica removed from crocidolite using four successive extractions.

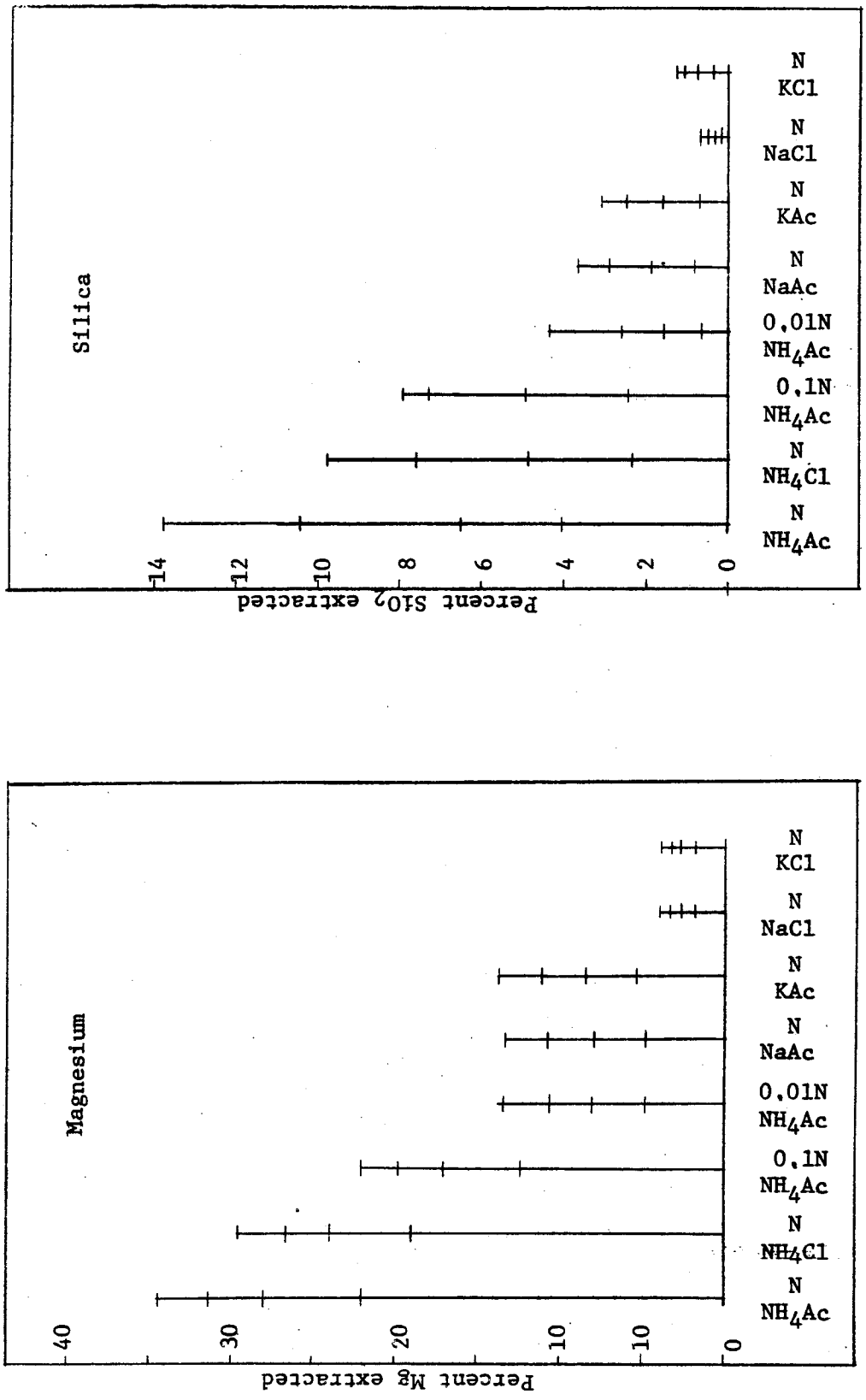

Figure 5, Magnesium and silica removed from chrysotile using four successive extractions,

breakdown and elapsed time of dissolution.[14] The extrapolations indicate that within a span of twenty years, which is the approximate incubation time of asbestosis, the greatest portion of cations leachable within this period of time are discharged from the fibers within the first year, the remainder being released slowly over the succeeding nineteen years.

No emperical correlations were found which would lend themselves to straight line plots of extraction time vs removal of silica and magnesium from the minerals in neutral salt solutions. However, the characterizations presented concerning the discharge of these constituents are thought to be valid.

References

1. Choi, I., "Kenetic Study of Dissolution of Asbestos Minerals in Water". Submitted to Journ. Colloid. Sci. for publication.

2. Malghan, S. G., "Dissolution Kenetics of Fibrous Amphibole Minerals in Water", M. S. Thesis, Mackay School of Mines, University of Nevada, 1971.

3. Luce, R. W., "Dissolution of Magnesium Silicates", Ph.D. Thesis, Stanford University, 1969.

4. Choi, I., op. cit. p. 8.

5. Clark, S. G., and Holt, P. F., "Studies of the Chemical Properties of Chrysotile in Relation to Asbestosis", Ann. Occup. Hyg., Vol. 3, 1961, p. 22.

6. Nagy, B., and Bates, T. F., "Stability of Chrysotile Asbestos", American Mineralogist, Vol. 37, 1952, p. 1055.

7. Badollet, M. S., "Asbestos, A Mineral of Unparalleled Properties", Journ. Can. Min. Met. Bull., Vol. 37, 1965, p. 237.

8. Gupta, A., "Reaction Rate Studies of Asbestos Minerals with Acids", M. S. Thesis, Mackay School of Mines, University of Nevada, 1971.

9. Gupta, S., Personal communication.

10. Allen, M., "Dissolution and Cation Exchange Studies of Asbestos Minerals in Aqueous Media", M. S. Thesis, Mackay School of Mines, University of Nevada, 1972.

11. Cralley, L. J., et al., "Characterization and Solubility of Metals Associated with Asbestos Fibers", Am. Ind. Hyg. Assoc. Journ., Dec. 1968, p. 171.

12. Dixon, J. R., et al, "The Role of Trace Metals in Chemical Carcenogenesis: Asbestos Cancers", Cancer Research, Vol. 30, 1968, p. 1068.

13. Mineral Research Progress Report, Department of Chemical and Metallurgical Engineering, University of Nevada, Reno, July 1971, p. 4.

14. Allen, M. op. cit., p. 34.

Special Studies in Electro-oxidation of Cinnabar*

S. Rudy and J. L. Hendrix

Most of the world's production of mercury comes from the direct furnacing of cinnabar ores. Pyrometallurgical methods are efficient in the sense that the mercury content of the calcine is usually very low. However, inherent losses in the condenser system are sometimes high (1) and thus unacceptable from a metallurgical as well as environmental standpoint. If air pollution due to the processing of mercury ores is to be avoided, a process that does not include sulfide furnacing is a logical choice.

One of the most promising hydrometallurgical schemes proposed in the last half-century is the chlorine/hypochlorite process initially patented by Glaeser(2) and recently made workable by Parks and Baker(3). Recoveries greater than 95% are possible from feed ranging from high grade cinnabar concentrates to very low grade ores. More recently, the United States Bureau of Mines (USBM) Reno Metallurgy Research Center has developed a hydrometallurgical process(4) for the extraction of mercury from cinnabar ores in which oxidation is accomplished by electrolysis of ore slurried with brine. Although the chemistry of the processes is similar, electrolytic oxidation differs from direct hypochlorite addition in that the chloride (Cl^-) concentration is substantially higher, which facilitates complex formation of the highly stable $HgCl_4^{-2}$ species. Bench and pilot scale investigations at the USBM have indicated extractions greater than 95% can be obtained with feed ranging from 0.6 to 20 pounds mercury per ton(4).

Important parameters in the electro-oxidation process include salt concentration, ore particle size, current density, treatment rate in amps per ton ore, electrode composition, electrode spacing and temperature(4).

EXPERIMENTAL:

Electro-oxidation tests were conducted on synthetic mixtures and naturally occurring cinnabar ores. The synthetic mextures used consisted of -35 mesh/+100 mesh purified silica sand, reagent grade mercuric sulfide (HgS), reagent grade sodium chloride (NaCl) and distilled water. Two naturally occurring ore types were studied; a hard opalitic ore from the Ivanhoe District containing 23.0 pounds Hg per ton, and a soft clay ore from the Cordero Mine containing 9.5 pounds Hg per ton. All tests were conducted by slurrying 1350 grams of -35 mesh ore and 300 grams of salt with 2500 ml of water. Current densities of 0.25 and 0.50 amperes per square inch, and treatment rates of 2.5 and 5.0 amperes were used. The electrodes were constructed of carbon, and the temperature was maintained at 30°C.

The analytical techniques employed in the investigation were as follows:

1. for $SO_4^=$: The standard barium chloride gravimetric method was used.
2. for OCL^- and ClO_3^-: A method furnished by the USBM utilizing an indirect iodometric titration with sodium thiosulfate was used.
3. for H^+: A corning model 12 pH meter was used.
4. for Mercury and Iron: The Reno Metallurgy Research Center conducted the analytical work for these species.

* This research was supported by U. S. Bureau of Mines Grant G0111058.

A brief description of the primary reactions that occur during the electrolysis of a neutral sodium chloride solution for the generation of hypochlorite(7) is necessary in order to understand the electro-oxidation process. Chloride ion is oxidized to chlorine at the anode.

$$2Cl^- \xrightarrow{-2e^-} Cl_2(aq)$$

which disproportionates in neutral solutions according to the equation

$$Cl_2 + H_2O \rightleftharpoons HClO + H^+ + Cl^-$$

Water is reduced at the cathode

$$2H_2O + 2e^- \rightarrow H_2\uparrow + 2OH^-$$

The reaction

$$Cl_2 + OH^- \rightarrow ClO^- + Cl^-$$

then takes place in the body of the solution, and the overall reaction is

$$Cl^- + H_2O \rightarrow ClO^- + H_2\uparrow$$

Figure 3 shows current potential curves for the system $Cl^-/Cl_2/ClO^-$ at a graphite electrode.

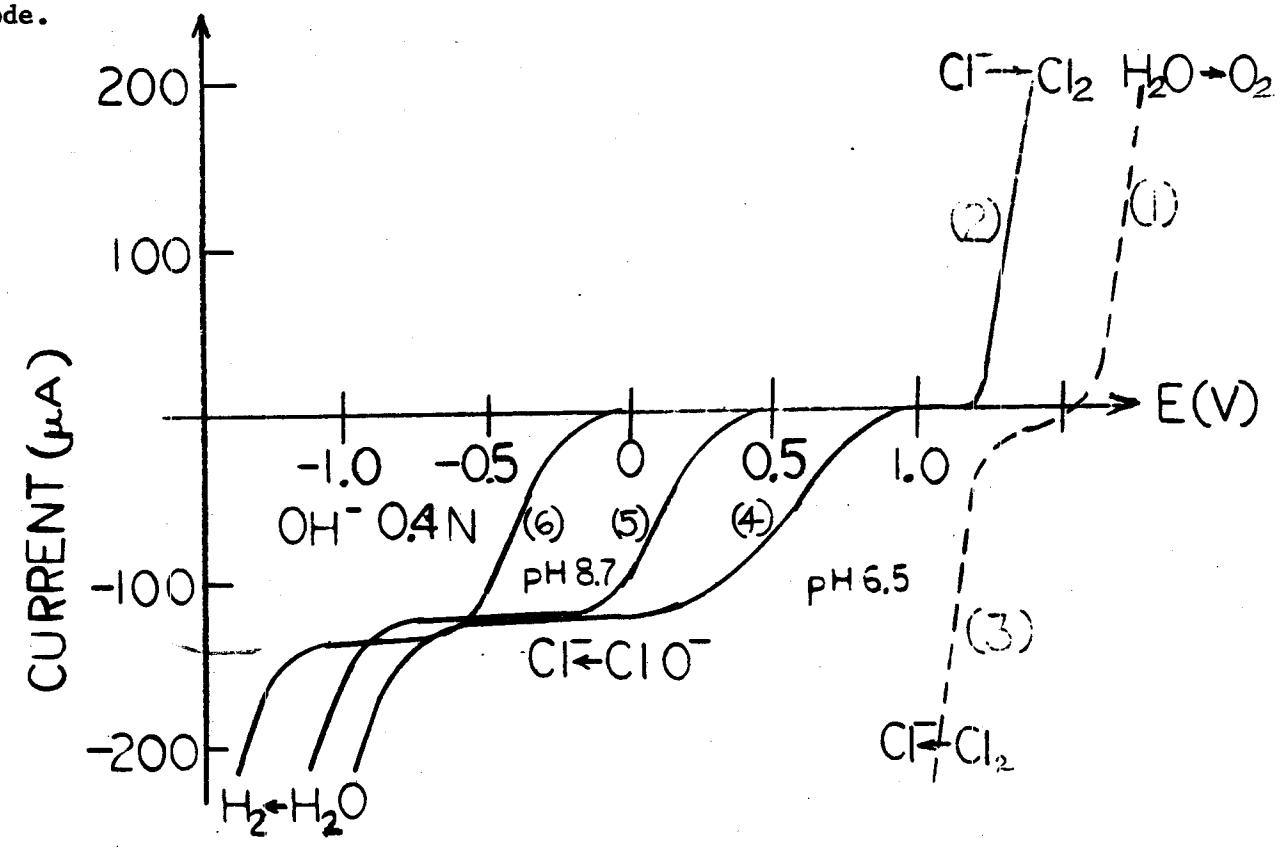

Fig. 3(7). The systems $Cl^-/Cl_2/ClO^-$ at a vibrating graphite electrode. Solutions: curve 1: N $HClO_4$; curve 2: M Cl^- + N HC 10_4; curve 3: saturated Cl_2 + N HC 10_4; curves 4, 5, 6: 4 x 10^{-3} M ClO^- + pH buffer.

THEORETICAL ASPECTS:

The most probable interaction between cinnabar and hypochlorite ion at a pH near neutrality is (5)

$$HgS + 4\ ClO^- \rightleftharpoons HgCl_2(aq) + 2\ Cl^- + SO_4^=$$

where ΔG° = -234.8 kcal/mole.

The thermodynamic free energy change associated with this reaction is so negative that it is effectively irreversible, i.e., no significant residual hypochlorite concentration is necessary to prevent the reverse reaction.

A distribution diagram for mercuric chloride complexes is shown in Figure 1. The diagram indicates that the $HgCl_4^{-2}$ complex predominates at a pCl of -0.3. The only other complex of significance is $HgCl_3^-$, and it is relatively minor.

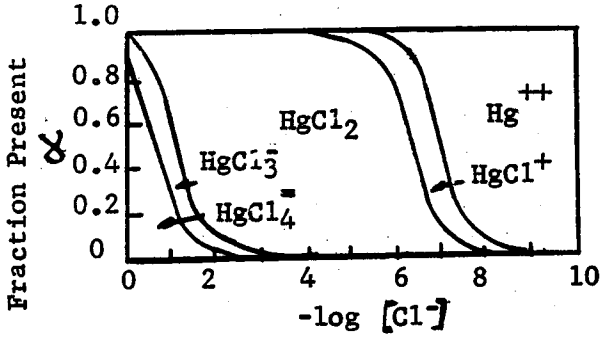

Fig. 1(6). Distribution diagram for mercuric chloride complexes. Note the very wide range over which $HgCl_2$ is the predominant complex.

The solubility of mercuric chloride in water is about 0.30 moles per liter(6), a phenomenon directly attributable to the formation of chloro complexes. A predominance-area diagram for solutions saturated with $HgCl_2$ is shown in Figure 2. It should be noted that the region in which HgO precipitates is shifted to the right for unsaturated solutions

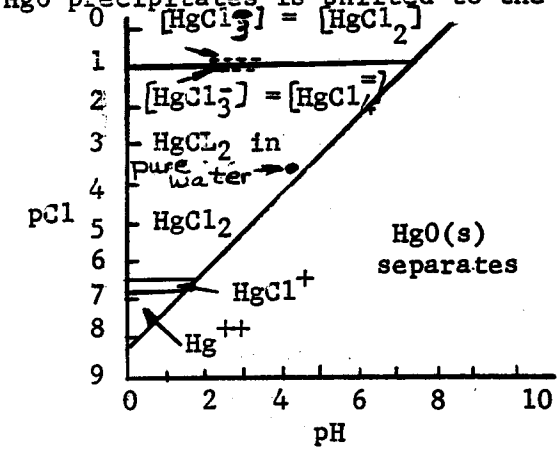

Fig. 2(6). Predominance-area diagram for solutions saturated with $HgCl_2$. The various regions indicate the values of pH and pCl for which a particular species predominates. To the right of the diagonal line, the solution is saturated with respect to both $HgCl_2$ and HgO. Note that $HgCl_3^-$ is never the predominant species.

DISCUSSION:

In all experiments, aqueous mercury concentration increased gradually at a decreasing rate until essentially all the cinnabar was consumed. In the case of synthetic ores, the reaction complexity was compounded by fluctuations in Hydrogen ion concentration, Figures 4-10, while in the case of naturally occurring ores such fluctuations were not encountered, Figures 11, 12. Naturally occurring ores displayed buffering characteristics considered optimum for the generation of hypochlorite. The addition of other oxidizable species, such as sulfur and pyrite, further compounded reaction complexity, and in the case of pyrite, caused electro-deposition of substantially all the aqueous mercury at the cathodes, Figures, 8, 9, 10.

Aqueous mercury concentration increased until essentially all the cinnabar was reacted, at which time the rates of formation of all other species exhibited dramatic changes under most of the conditions tested.

Concurrent to the reaction in which cinnabar is consumed by hypochlorite, a reaction in which mercuric or mercuric complexes are reduced to elemental mercury must be proposed. The reduction is due to direct reduction at the cathode, however, a mechanism as previously proposed by Korinek and Halpern(8) may also be encountered. Elemental mercury was observed in the cell residue and on the cathodes in all tests.

The fluctuation in hydrogen ion observed with synthetic ore samples can be explained as follows. Initially the distilled water has a pH of just under 6.0. The solution becomes basic due to the generation of hydroxyl ion at the cathode. Acid is generated as the reaction between mercuric species and hydrogen gas proceeds(8) until all the cinnabar has been reacted, after which time the solution returns to a pH near neutrality.

The residual concentration of hypochlorite remains small until all the cinnabar is reacted and the pH of the solution increases to the extent that hypochlorite is stable in solution, i.e., the reaction $HClO + Cl^- + H^+ \; Cl_2 + H_2O$ occurs under acid conditions(9).

Sulfate concentration increases with an apparent constant rate until all the cinnabar has reacted. A marked decrease in the rate of formation occurs at that time. However, sulfate concentration continues to increase due to the oxidation of colloidal sulfur.

Chlorate concentration remains insignificant in all synthetic ore tests, with the exception of that test corresponding to Figure 6, in which the system was buffered with 0.1 Molar $NaHCO_3$.

The effects of the addition of pyrite to synthetic ore is evident from viewing Figures 8, 9, 10. The significant effect is the formation of ferric-mercuric-chloro complexes, $FeHgCl_4^+$, which are apparently more electro active than $HgCl_4^=$ complexes, with subsequent electrodeposition at the cathode. Large quantities of acid and sulfate are produced due to the oxidation of pyrite. Hypochlorite does not become significant due to the extreme acid conditions. Chlorine gas is the primary oxidant under such acid conditions.

Figures 11 and 12 show the results of electro-oxidation test conducted with naturally occurring ores. As previously mentioned, the ores are well buffered. The same general trends occur in regard to all other species with the exception of hypochlorite.

Table I shows the optimum results tabulated for all experiments.

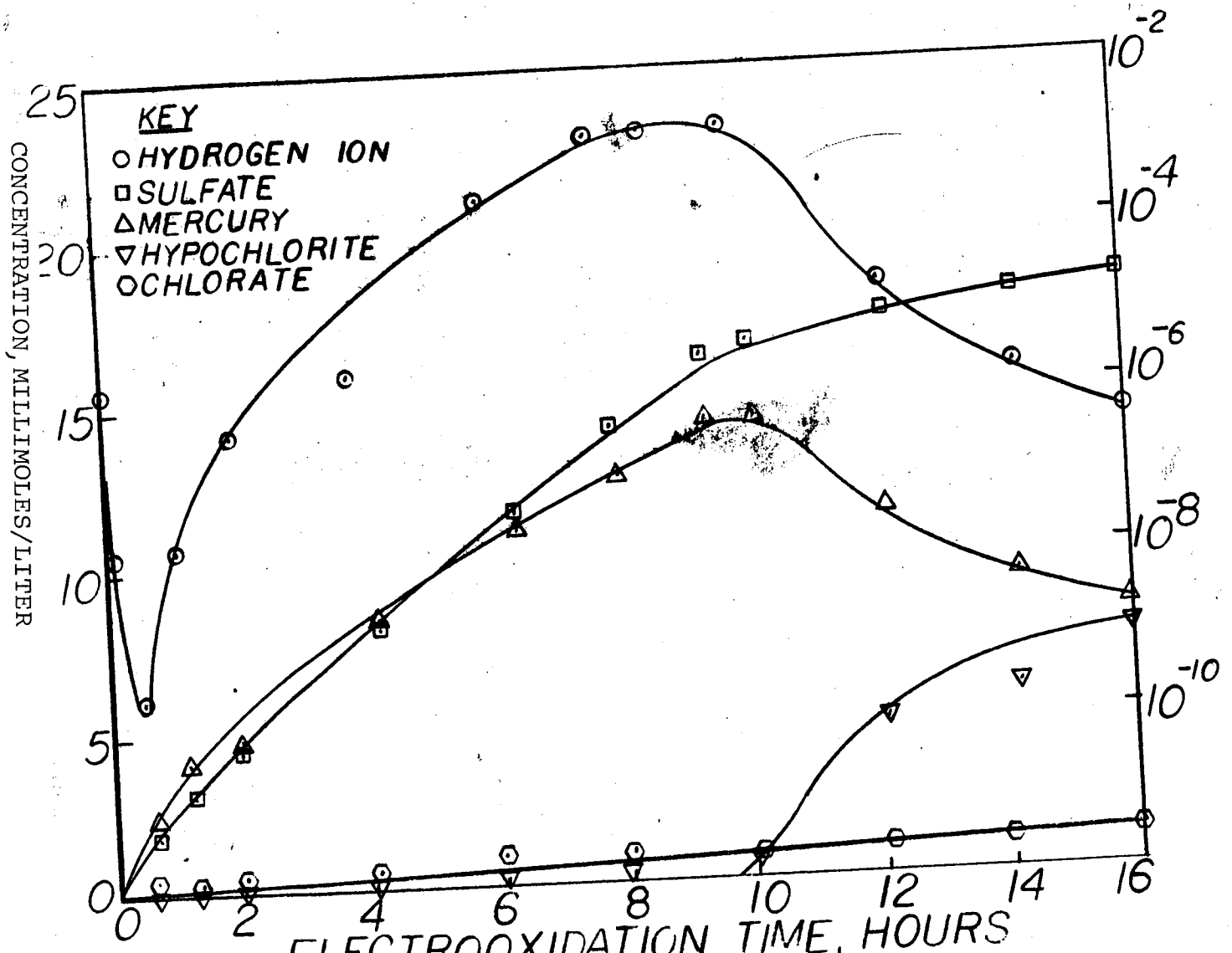

FIGURE 4. ELECTROLYTIC OXIDATION OF A 1% HgS SYNTHETIC ORE AT 0.25 AMPS PER SQ. IN., 2.5 AMPS, 30 °C.

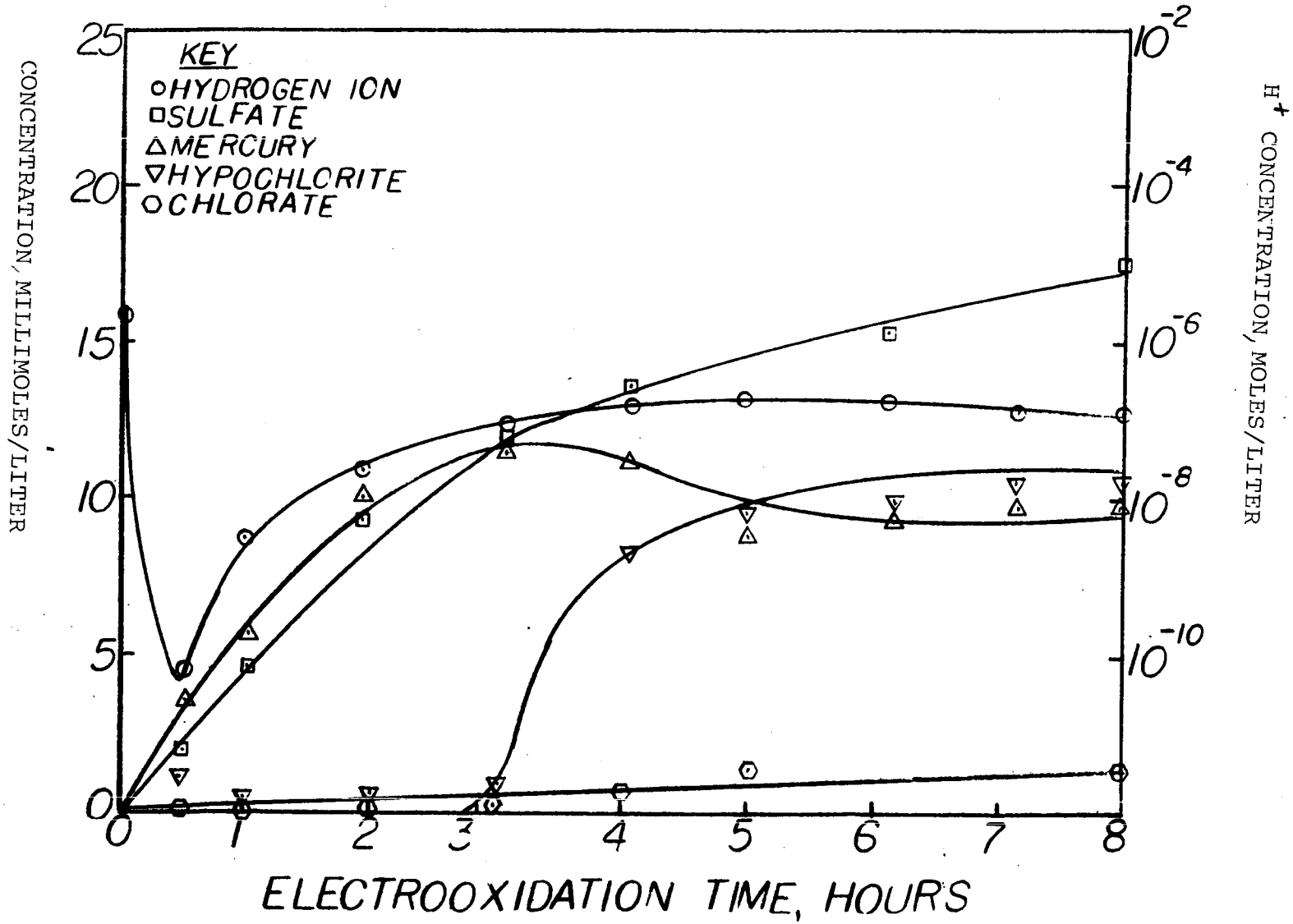

FIGURE 5. ELECTROLYTIC OXIDATION OF A 1.0% HgS SYNTHETIC ORE AT 0.5 AMPS PER SQ. IN., 5 AMPS, 30°C

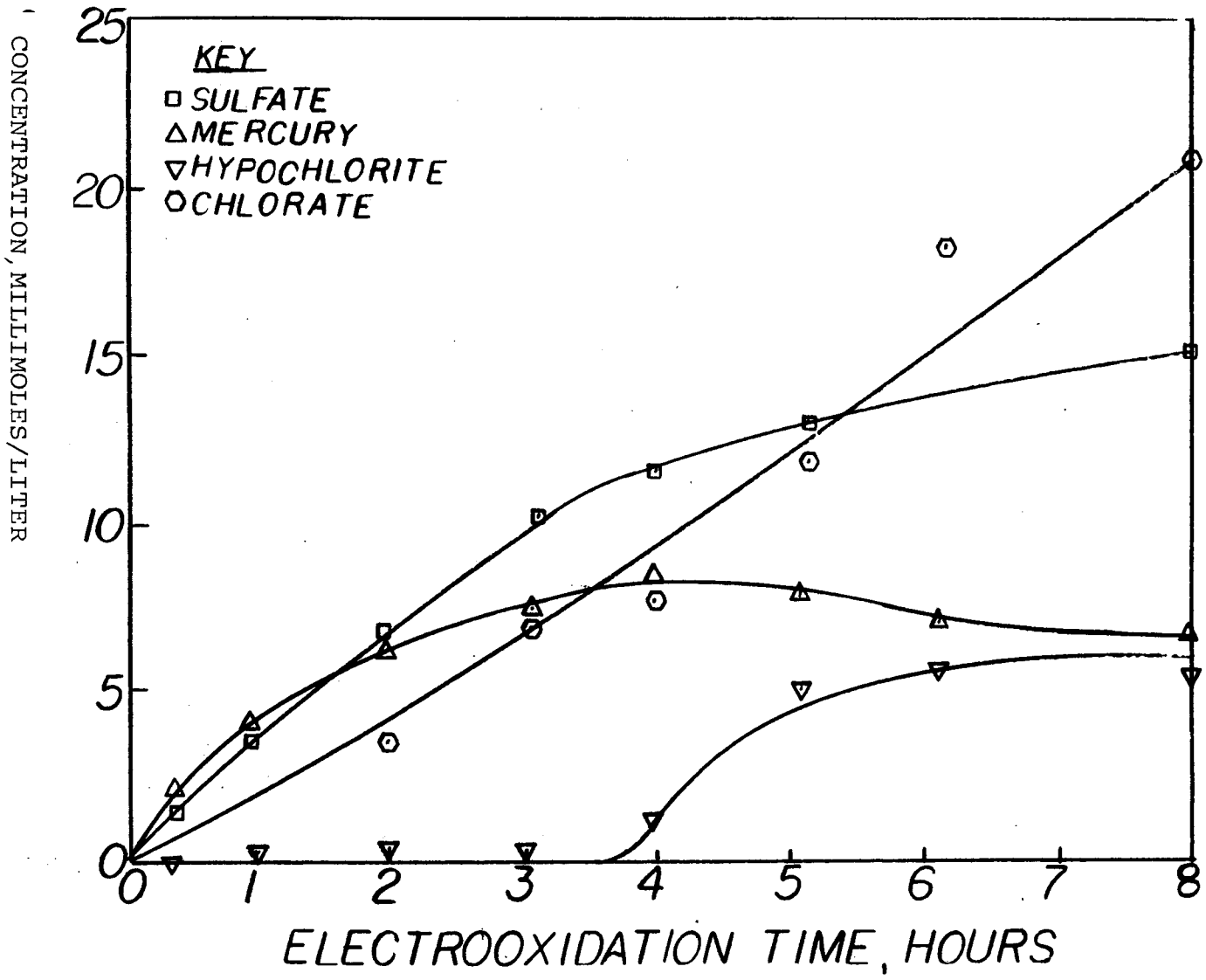

FIGURE 6. ELECTROLYTIC OXIDATION OF A 1.0% HgS SYNTHETIC ORE BUFFERED AT pH 8.2 WITH $NaHCO_3$ AT 0.5 AMPS PER SQ IN, 5 AMPS, 30°C

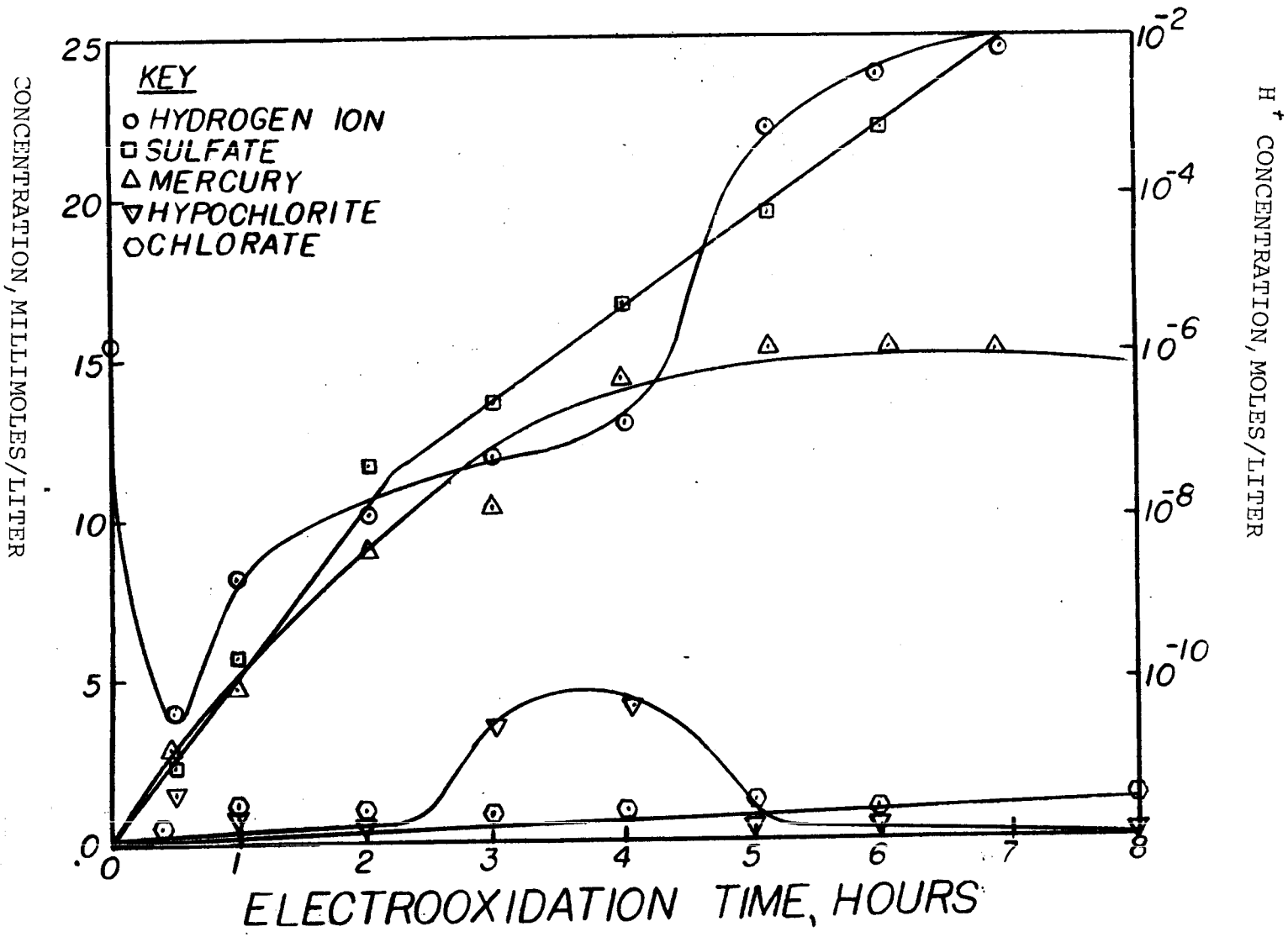

FIGURE 7. CONCENTRATION CURVES FOR THE ELECTROLYTIC OXIDATION OF A 1.0% HgS - 1.0% SULFUR SYNTHETIC ORE AT 0.5 AMPS PER SQ. IN., 5 AMPERES, 30°C

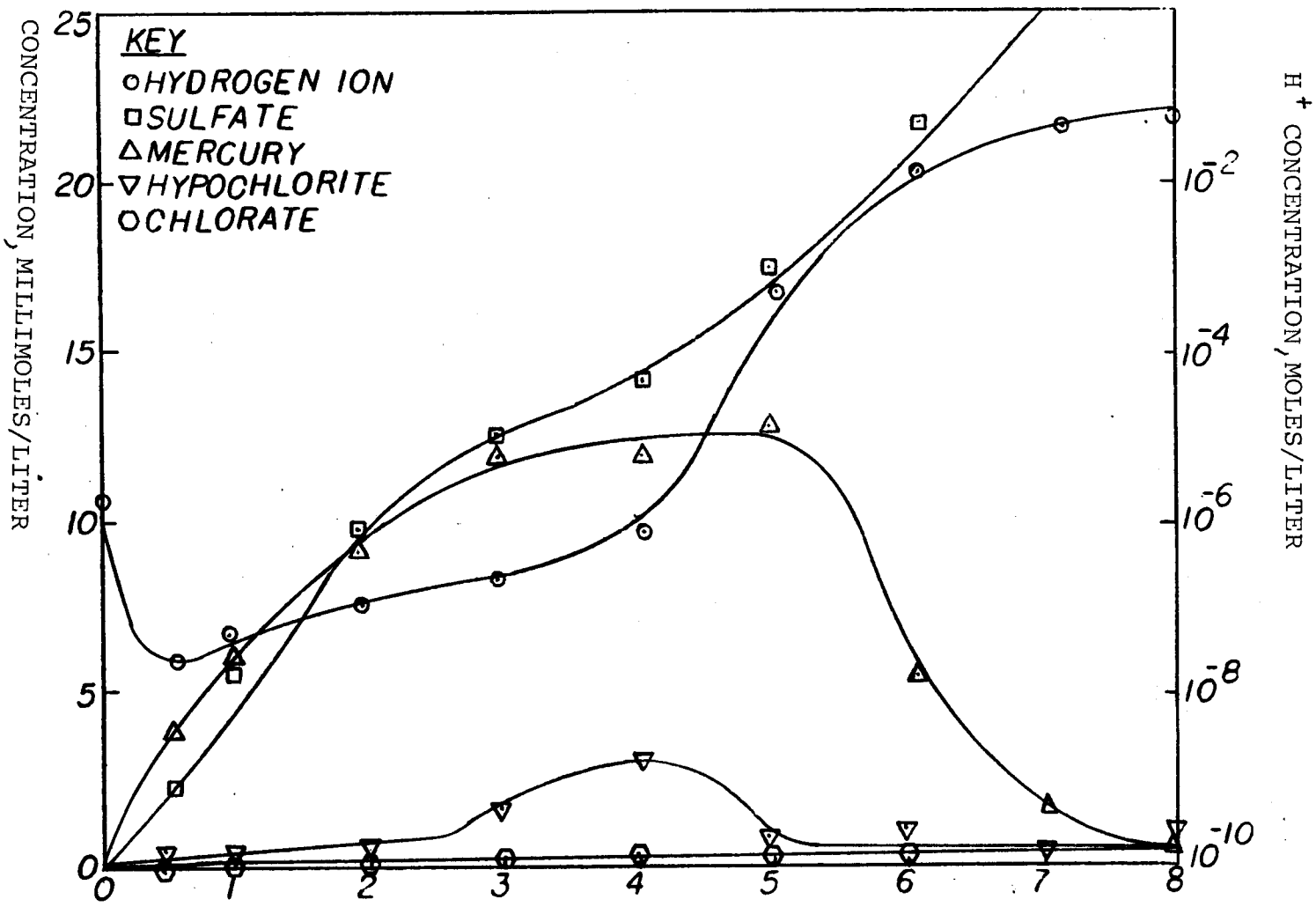

FIGURE 8 CONCENTRATION CURVES FOR THE ELECTROLYTIC OXIDATION OF A 1.0% HgS - 1.0% FeS_2 SYNTHETIC ORE AT 0.5 AMPS PER SQ. IN., 5 AMPERES, 30°C

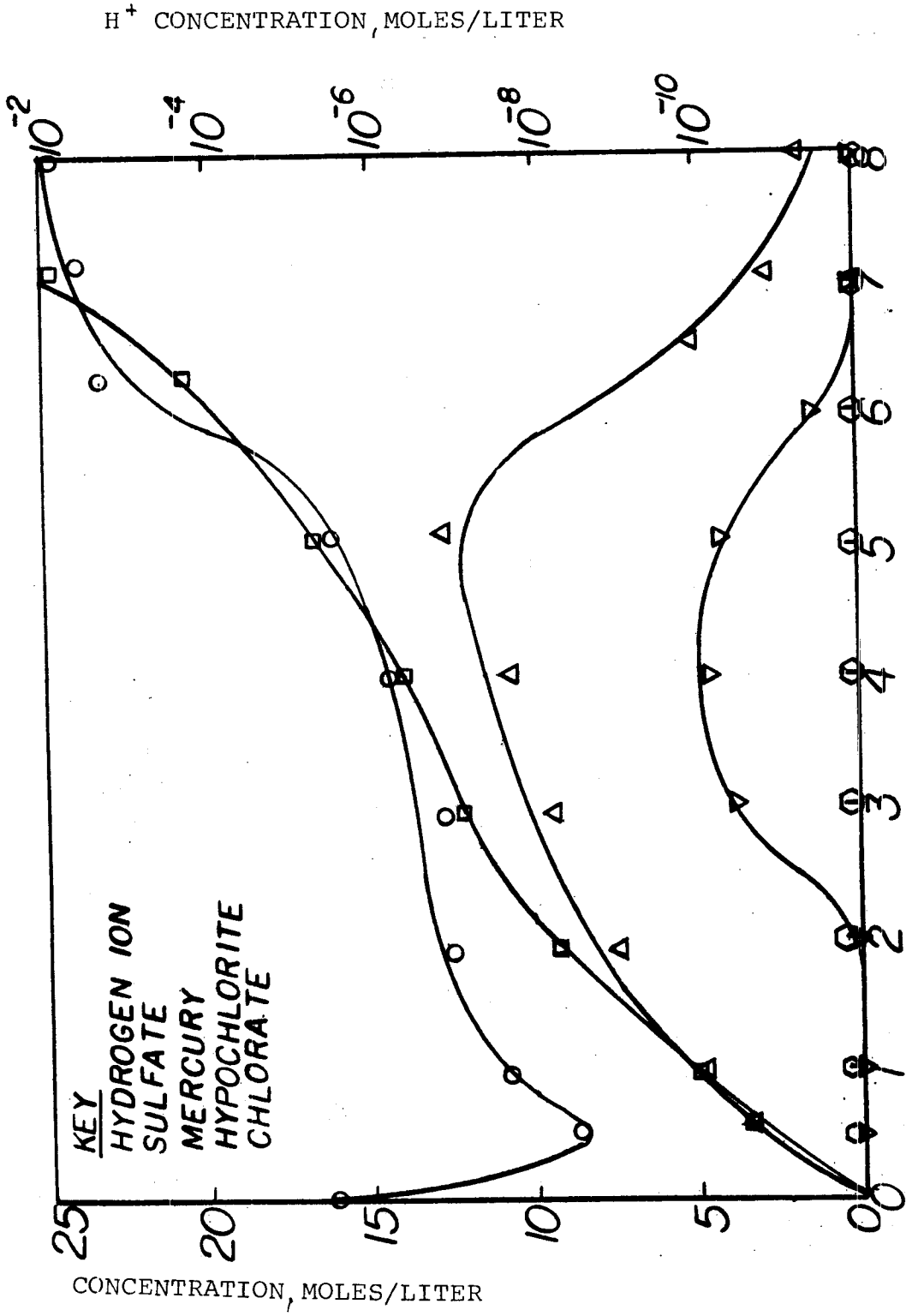

FIGURE 9. ELECTROLYTIC OXIDATION OF A 10% H_6S-0.6% FeS_2 SYNTHETIC ORE AT 0.5 AMPS PER SQ IN., 5 AMPS, 30°C

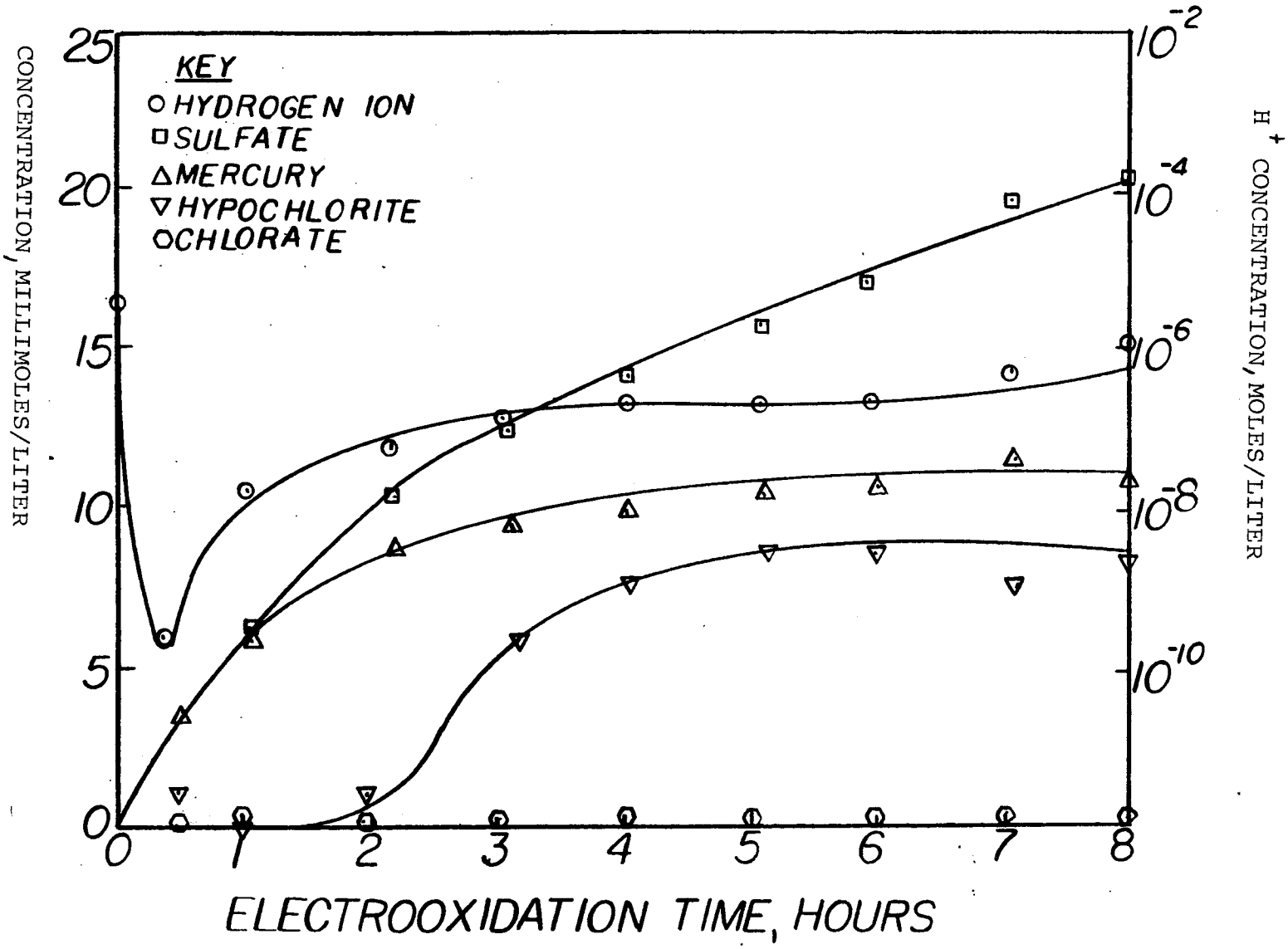

FIGURE 10. ELECTROLYTIC OXIDATION OF A 1.0% HgS-0.2% FeS_2 SYNTHETIC ORE AT 0.5 AMPS PER SQ. IN., 5 AMPS, 30°C

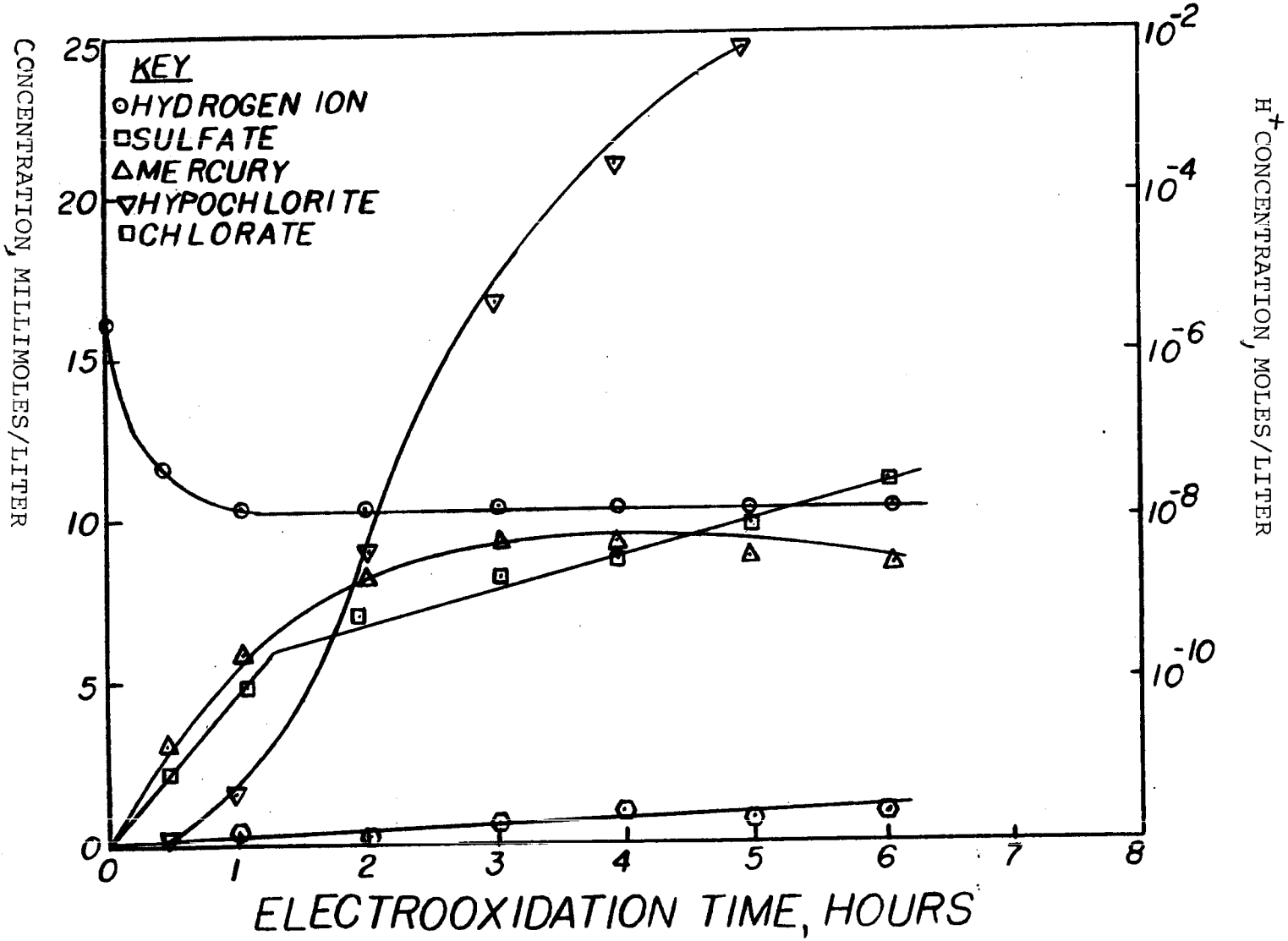

FIGURE 11. CONCENTRATION CURVES FOR THE ELECTROLYTIC OXIDATION OF CORDERO ORE CONTAINING 0.55% HgS AT 0.5 AMPS PER SQ. IN., 5 AMPERES, 30°C

FIGURE 12. CONCENTRATION CURVES FOR THE ELECTROLYTIC OXIDATION OF IVANHOE ORE CONTAINING 1.33 % H_2S AT 0.5 AMPS PER SQ. IN., 5 AMPS AT 30°C

TABLE I

Tabulated Optimum Results for Figures 4 through 12

Test Corresp. to Figure No.	Maximum Conc. of Hg in solution millimoles/liter	Correspond. $SO_4^=$ Concentration millimoles/liter	Maximum % Hg Originally contained in the Feed Present in Solution	*Correspond. % $SO_4^=$ Present in Solution
4	14.0	16.4	60	72
5	11.9	11.9	52	52
6	8.6	11.4	38	49
7	19.6	15.0	64	--
8	12.8	16.5	55	--
9	12.9	16.3	55	--
10	11.1	19.2	48	--
11	9.2	8.6	67	32
12	13.2	19.2	43	81

* Assuming all sulfate is derived from HgS.

Bibliography:

1. Duschak, L. H., Trans. AIME, 91, 283, 1930

2. Glaeser, W., Method of Producing Mercury, U. S. Pat. 1, 637, 481, Aug. 2, 1927.

3. Parks, G. A., and Baker, R. E., Mercury Process, U. S. Pat. 3,476,552, Nov. 4, 1969.

4. Scheiner, B. J., Lindstrom, R. E., Shanks, D. E. and Henrie, T. A., "Electrolytic Oxidation of Cinnabar Ores for Mercury Recovery."

5. Parks, G. A. and Fittinghoff, N. A., EMJ, 171, 107, June (1970).

6. Butler, J. N. Ionic Equilibrium - A Mathematical Approach, Addison-Wesley Publishing Company, Inc., Palo Alto, 1964.

7. Charlot, G., Badoz-Lambling, J., and Tremillon, B., Electrochemical Reactions, Elsevier Publishing Company, Amsterdam, 1962.

8. Karinek, G. J. and Halpern, J., J. Phys. Chem., 60, 285, (1956).

9. Latimer, W. M., Oxidation Potentials, Prentice-Hall, Inc., New York, 1952.

Analysis of Asbestos Minerals using a Van de Graaff Generator*

by: D. D. Sharma

Introduction

Total chemical analyses of asbestos minerals such as chrysotile, amosite and crocidolite are difficult[1]. Trace element determinations are particularly hard to perform. This study investigates the use of a relatively new analytical method for the performance of trace metal analyses of asbestos minerals. The method is based on x-ray emission induced by the passage of energetic protons through mineral samples.

Recent work[2-5] has indicated that a high degree of sensitivity can be achieved in trace element analyses of various samples using heavy charged particles as the means of inducing x-ray emission. Besides high sensitivity the method has certain advantages over techniques such as atomic absorption and colorimtry in that many trace element analyses can be performed in a single run and the method is non-destructive.

The degree of sensitivity that can be achieved in x-ray analysis of samples is directly proportional to the x-ray excitation cross section. By measuring K x-rays induced by 1.5 Mev protons, Johansson et al[1], have reported detecting as little as 4×10^{-11} gm of titanium and 8×10^{-10} gm of copper. A study of the sensitivity as a function of the atomic number has shown that the sensitivity of the method is maximum in the region of transition elements. This fact makes the technique particularly suitable for trace element analyses of asbestos minerals since most of the trace metals of interest associated with these minerals are transition metals.

Experimental Apparatus

A schematic diagram of the experimental arrangement is given in Fig. 1. A proton beam of 1.5 Mev energy from the Van de Graaf generator is focussed to about 1 cm diameter and then deflected in to the target chamber. After passing through the target, the proton beam continues on into a Faraday cup. A digitized current integrator connected to the Faraday cup is used to measure the beam current. As many as twelve targets may be placed in the bombardment position in the center of the chamber. The target placed in the bombardment position automatically makes an angle of 45° with respect to the beam and detector axes.

The x-ray spectra emitted from the targets are measured by a semiconductor spectrometer. The spectrometer consists of an evacuated cryostat, a Si(Li) detector and an internally mounted FET (field effect transistor). Both the detector and the FET are operated at liquid nitrogen temperature. The electrical pulses generated by the absorption of x-rays in the detector are taken from the output of the preamplifier. A linear amplifier is used to amplify these pulses. Finally the pulses are analyzed by a 512 channel pulse height analyzer. The energy resolution of the whole system is 0.20 KeV FWHM for the Fe K x-rays under the conditions of the experiment.

* This research is supported by Department of Health Education and Welfare Research Grant EC00381

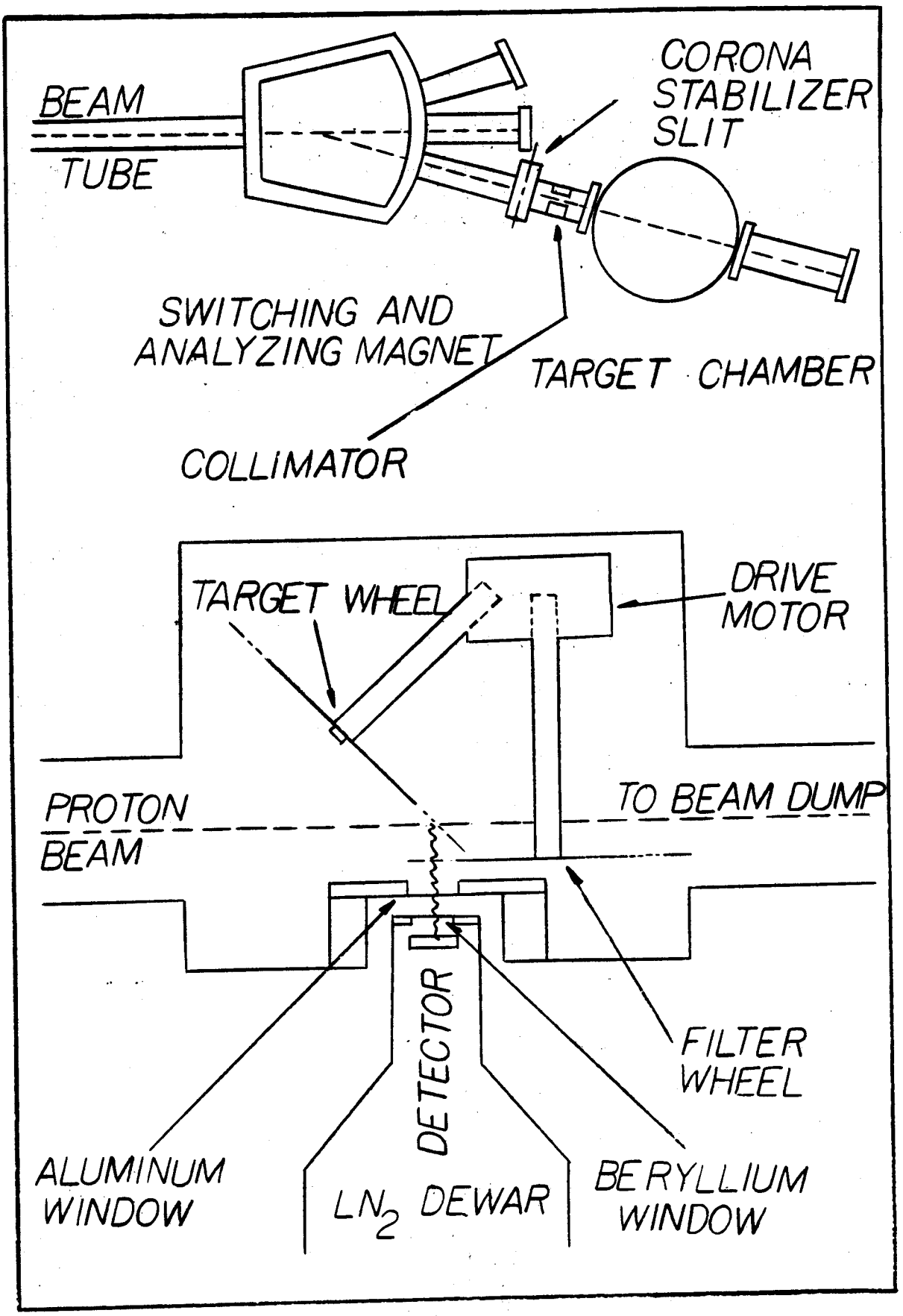

FIGURE 1. SCHEMATIC DIAGRAM OF THE EXPERIMENTAL ARRANGEMENT

Experimental Procedure

The minerals studied included chrysotile from Thetford mines, Quebec, amosite from South Africa and crocidolite from South Africa. In order to measure the total amounts of trace elements, 5.00 gm of each mineral was weighed and digested with con. HF three times. The minerals were then digested with HCl and filtered (# 42 Whatman). The solutions were then diluted so that the solutions analyzed contained 5 mg/ml of the minerals. Amosite and chrysotile were also dissolved in Con. HCl and solutions prepared for determining the extent to which trace elements are dissolved by HCl digestion. From these solutions, 20 λ aliquotes were withdrawn, deposited on mylar backings and evaporated to dryness. The evaporation of samples was carried out in an evacuated desiccator to minimize the contamination of the samples. Standard samples from solutions containing V, Mn, Cr, Fe, Co, and Ni at 0.1, 1.0, and 10.0 PPM concentrations were also prepared.

The unknowns as well as standard targets are mounted on the target wheel and placed in the scattering chamber. A proton beam of 1.5 Mev energy is then passed through each target and the resulting characteristic x-ray spectra are recorded. For each target the data are normalized to 100 microcoulomb of integrated proton beam.

Data Analysis

The x-ray spectra are analyzed by computing the net counts in the x-ray peak contributed by a particular element present in the target. Since the background varies from peak to peak, it was decided to subtract a linear background from each x-ray peak to get the net counts. Only K_α lines are used in computations. The presence and intensity of K_β lines is used for rejecting interferences.

The number of counts N_x in the x-ray peak corresponding to M gm of an element present in the sample is given by

$$N_x = (M/A) N_o \sigma_x w \epsilon n \left(\frac{\Omega}{4\pi}\right) \qquad (1)$$

where,

A = Atomic Weight,

N_o = Avogardro's number,

σ_x = ionization cross section,

w = fluorescent yield,

ϵ = detector efficiency,

n = number of protons/cm^2 incident on the target,

and $\frac{\Omega}{4\pi}$ = solid angle subtended by the detector.

By counting the number of x-rays N_x in a peak, one can measure the unknown mass M of an element present in the sample. All other parameters in equation (1) are either measured or can be obtained from published reports. Because of uncertainties in the values of ionization cross sections and fluorescent yields, it is preferable to make relative measurements. For this purpose standard samples are activated along with unknown samples and the unknowns are measured by comparison.

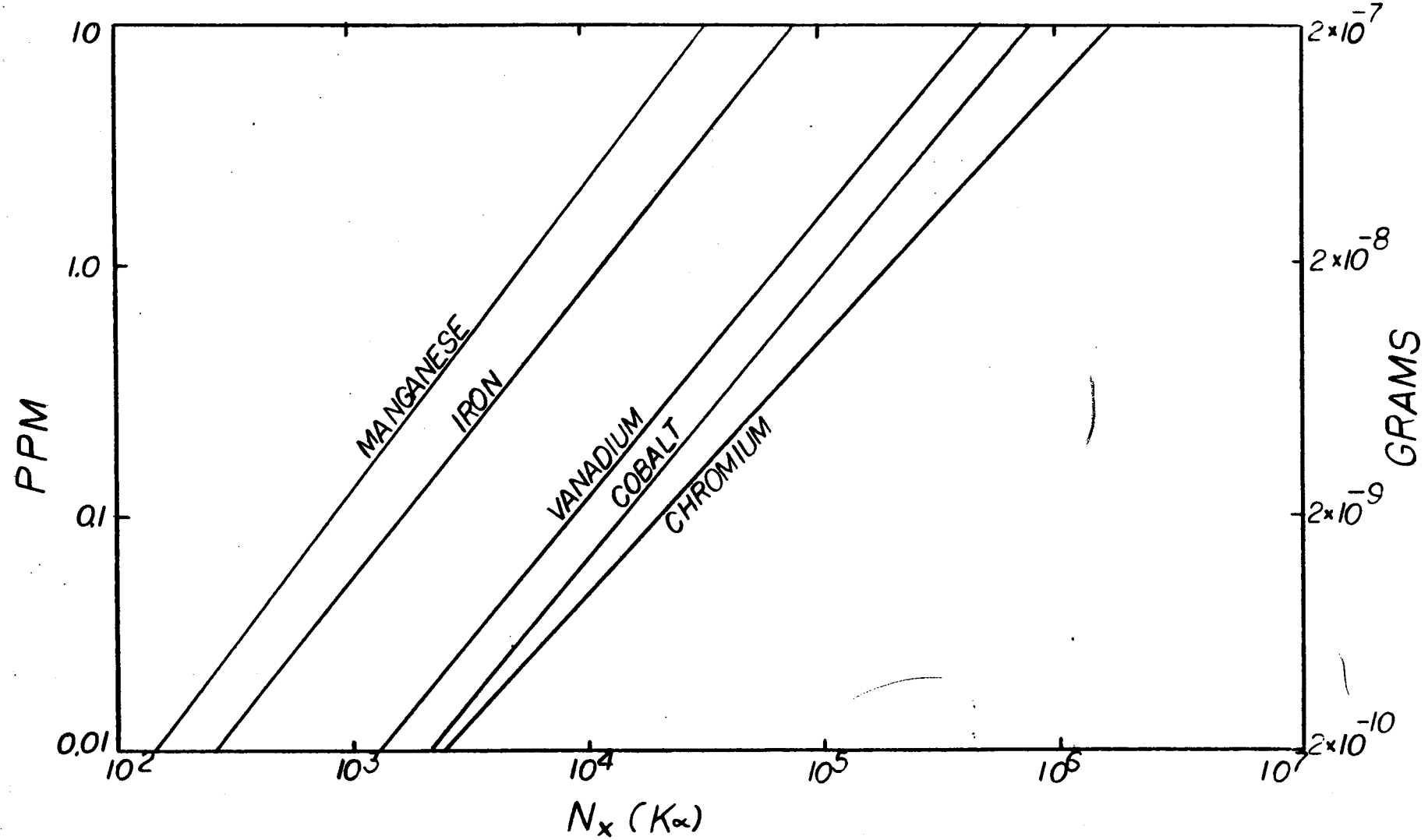
10
1.0
0.1
0.01
PPM
MANGANESE
IRON
VANADIUM
COBALT
CHROMIUM
10^2
10^3
10^4
10^5
10^6
10^7
N_x (Kα)
2×10^{-7}
2×10^{-8}
2×10^{-9}
2×10^{-10}
GRAMS

FIGURE 2.

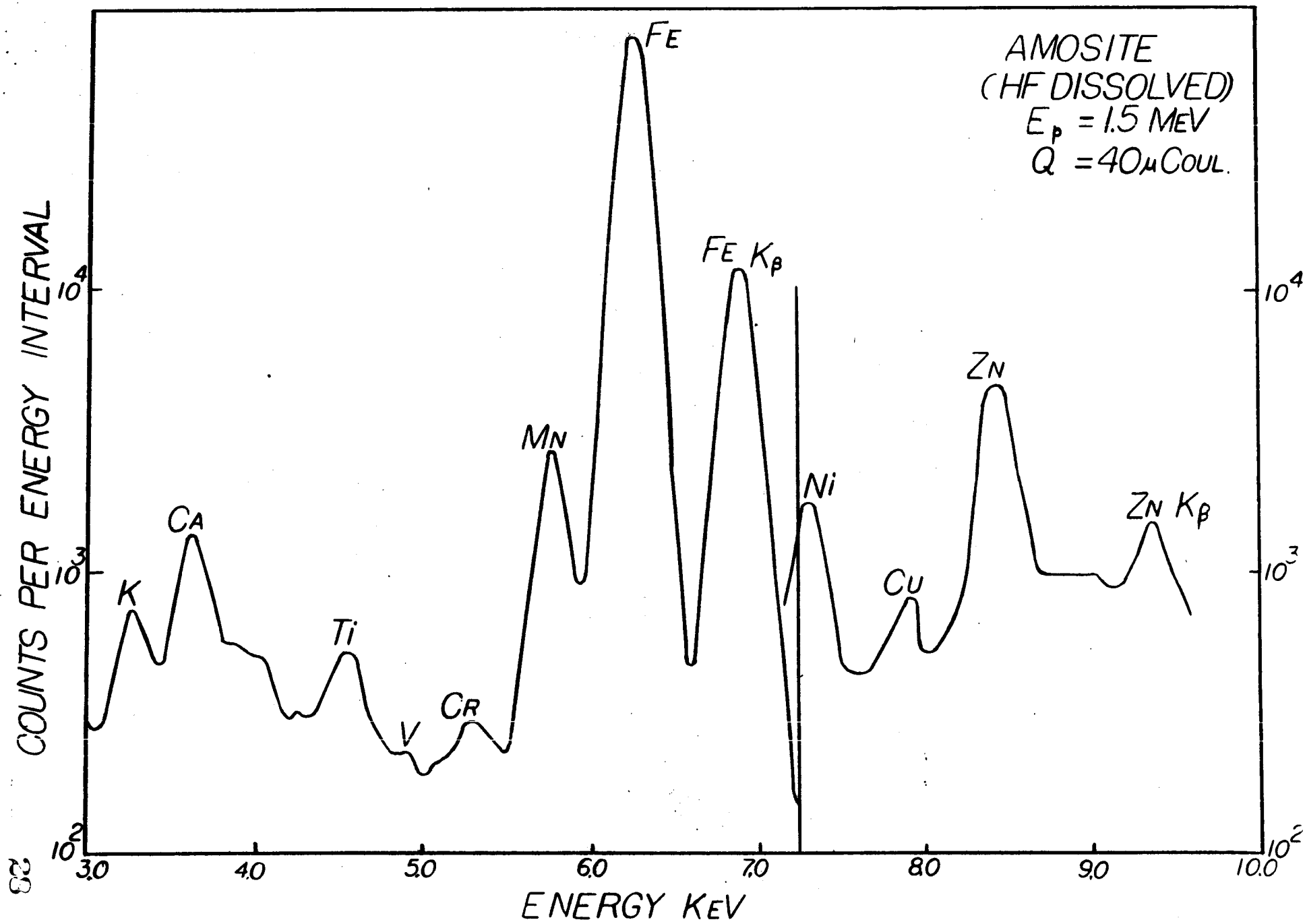

FIGURE 3. X-RAY SPECTRUM OF AMOSITE

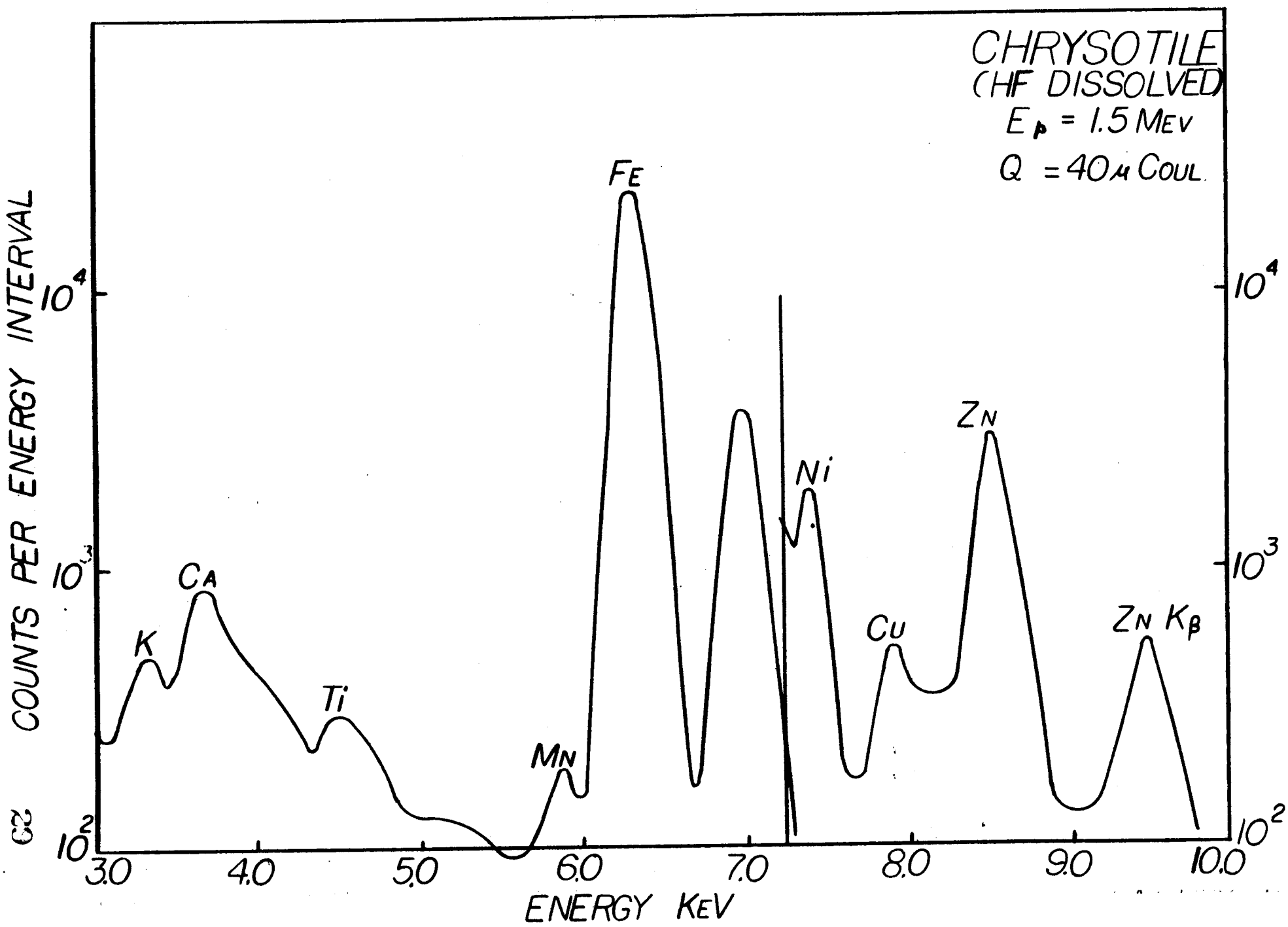

FIGURE 4. X-RAY SPECTRUM OF CHRYSOTILE

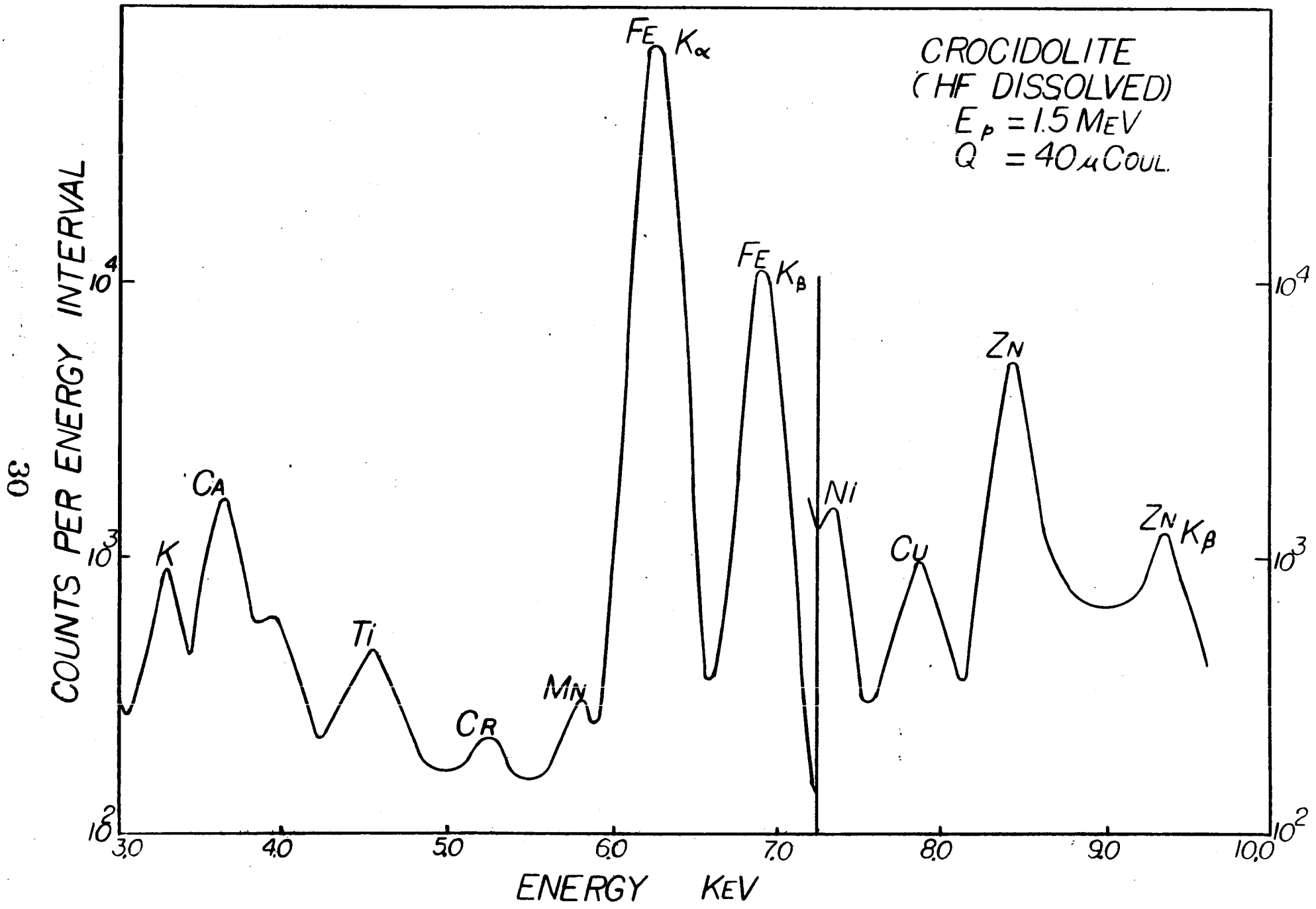

FIGURE 5. X-RAY SPECTRUM OF CROCIDOLITE

TABLE I

Trace Element Concentration in Asbestos Minerals (%).
Digested with HF

Element	Amosite	Chrysotile	Crocidolite
K	0.088	0.046	0.115
Ca	0.140	0.057	0.165
Ti	0.061	0.029	0.090
Cr	0.010	0.002	0.007
Mn	1.160	0.030	0.058
Fe	32.00	8.20	28.00
Ni	0.053	0.055	0.034
Cu	0.001	0.002	0.010

TABLE II

Trace Element Concentration in Amosite and Chrysotile
Digested with con. HCl (%)

Element	Amosite	Chrysotile
K	0.050	
Ca	0.150	
Sc	0.007	
Ti	0.105	0.040
V		0.007
Cr	0.005	0.005
Mn	1.140	0.036
Fe	30.03	9.50
Ni	0.002	0.009
Co		0.0002
Cu	0.030	0.075

Results and Conclusions

The results discussed here are of a preliminary nature as only a few measurements of trace elements in asbestos minerals (using this technique) have been made so far. Some time has been devoted to making measurements on standard samples. In Fig. 2 calibration graphs for V, Cr, Mn, Fe, and Co are shown. The net counts in the K_{α} peaks of these elements obtained for concentrations in the range 0.1 PPM to 10.0 PPM are plotted. Extrapolation of these curves allows one to determine any concentration in the range from 0.01 PPM to 100.0 PPM.

In Fig. 3 is shown a x-ray spectrum of amosite digested with con. HF. From this figure it is clear that K, Ca Ti, V, Mn, Fe, Ni, and Cu are present in amosite, besides other low Z elements not shown in the figure. The concentrations of these elements in amosite are given in Table I. Figures 4 and 5 show the x-ray spectra obtained from chrysotile and crocidolite minerals, also digested with con. HF. The concentrations of various trace elements in chrysotile and crocidolite minerals are given in Table II. The x-ray spectra of chrysotile and amosite minerals digested with con. HCl were also recorded. The results are given in Table II. The concentrations of trace elements given in tables I and II are in good agreement with other reported results[6]. It should be noted, using other methods, that measurements of copper have not been generally reported.

In conclusion it is reasonable to say that this method is competitive with neutron activation, atomic absorption and x-ray fluorescence techniques for making trace element analyses. A major advantage which this method offers is that all the elements with $Z > 11$ may be simultaneously measured in a single run. The sensitivity of the method is relatively high for trace element analysis in transition metals region using K x-rays and for high Z elements using L x-rays. The method is especially suitable for the following type of studies of asbestos minerals:

1. Aging studies of dissolution of trace elements in various solvents.

2. pH of a solution is an important property and amounts of trace elements in a solution vary with changes in pH. Thus, a study of trace element concentration as a function of pH could easily be accomplished using the technique.

3. It has been found that asbestos causes lung canter[7]. It is possible that the trace metals present in asbestos contribute significantly in causing lung cancer. A study of the solubility of asbestos trace metals in water at human body temperature and in pH range 6.7 to 7.4 might be quite interesting.

References

1. Johansson, T. B., et. al., Nucl. Instru and Meth. 84 (1970) p141.

2. Watson, R. L., et al., Nucl. Instr. and Meth. 93 (1971) p69.

3. Flocchini, R. G., et al., Submitted to Nucl. Instr. and Meth. 7/71.

4. Sharma, D. D., Ph.D. Thesis, University of Nevada 1971.

5. Application of Nuclear Physics Techniques to Trace Element Analysis. Talks presented at the APS meeting 11/71.

6. Allen, M., Mineral Research Progress Report, July 1971, Dept. of Chemical and Metallurgical Engineering, Univ. of Nevada, Reno.

7. Chemical Abstract 1077204 (1970).

Adsorption of Carboxylic Groups on Fe_2O_3*

by: Salim Akhtar and Satish Kumar Khanna

Introduction

The study of adsorption of ions and molecules at the mineral-water interface is important in mineral processing for many reasons. Flotation, flocculation and dispersion are a few areas where the behavior of particulate solids depends upon the adsorbed molecules and ions at the solid-liquid interface. The studies on adsorption are often conducted by indirect methods such as electrophoresis and streaming-potential measurements. Infrared spectroscopic methods present the possibility of direct observation of adsorbed species. However, there are many difficulties which have to be overcome before the IR-spectroscopy can become a routine tool for the adsorption studies.

Transmission spectroscopic methods usually need some kind of medium for the samples, and often nujol or alkali-metal halides are used for this purpose. Partly because of the difficulties arising from the interaction of the samples with the media, and partly because of the small quantities of the samples (e.g., up to 0.5% in KBr), the adsorbed species are difficult to observe with transmission spectroscopy. Attenuated Total Reflection (ATR) spectroscopy seems a promising alternate method. The objectives of this investigation are two-fold: to explore the usefulness of ATR methods for adsorption studies; and to investigate the adsorption of ions and molecules at the mineral-water interface in several systems of interest.

In the present phase of this study the adsorption of a new class of collectors, the amphoteric surfactants, on hematite is being studied. The particular amphoteric surfactants studied are amino-acids and contain both carboxylic and amine groups. This report presents the study of the adsorption of carboxylic groups on Fe_2O_3 and hematite.

Adsorption of Carboxylic Groups

Fatty Acids

Fatty acids, such as oleic acid, are used as collectors for many oxide minerals. It is commonly believed that carboxylic group (-COOH) of the fatty acids adsorbs on the mineral surface. Peck et al.[1] have shown, with transmission spectroscopy, that oleic acid chemisorbs on hematite through COO^- radical, and the C = O stretching band of -COOH which is at 1705 cm^{-1} is replaced by a band between 1540 cm^{-1} and 1520 cm^{-1}.

We have examined the adsorption of carboxylic groups on Fe_2O_3 and hematite with ATR, using a Beckman IR-10 Spectrophotometer. The double beam mode of the IR-10 was used in all our work, and an attenuator was placed in the reference beam to compensate for the low intensities which are common in ATR. The adsorption of carboxylic groups of acetic acid, oleic acid and glycine on Fe_2O_3 and hematite were studied.

Adsorption of Acetic Acid: The spectra of glacial acetic acid (manufactured by Du Pont) was obtained by coating it on a germanium reflection plate. The spectra show many broad bands with shoulders. The bands due to -COOH are listed in Table I.

* This research is supported by U.S. Bureau of Mines project G0110303.

Table I. Adsorption Bands of Carboxylic Group in Acetic Acid with ATR

Observed band (cm^{-1})	Assignment	Reference
1750	C = O stretch	(2)
1400	OH deformation in plane	(2)
1280	C-O stretch	(2)
1190	COH bending	(3)

The adsorption of acetic acid on Fe_2O_3 (99.5%, from J. T. Baker Co.) was carried out in two ways.

(i) The Fe_2O_3 was heated in air to 750°F for one hour and exposed to acetic acid acid vapors in a closed vessel for one-half hour.

(ii) The Fe_2O_3 was heated in an aqueous solution of acetic acid at pH 2.7 for one hour at 200°F, filtered, and dried at 150°F for 12 hours.

The spectra of Fe_2O_3 exposed to acetic acid vapors are similar to those of acetic acid but weaker and additional bands at 1580 cm^{-1} and 1420 cm^{-1} appear. Subsequent heating of these samples for 12 hours at 150°F, gives spectra which show only two broad bands at 1560 cm^{-1} and 1400 cm^{-1}.

The spectra of Fe_2O_3 heated in aqueous solution of acetic acid, are similar to those exposed to acetic acid vapor, except that the band at 1750 cm^{-1} is missing, and the band at 1580 cm^{-1} has shifted to 1550 cm^{-1} and become stronger. Other bands in the range 1190 cm^{-1} to 1280 cm^{-1} are very weak.

Adsorption of Glycine: Glycine is the lowest molecular weight representative of amino acids. The ATR spectra of glycine is very weak and was interpretable only by comparison with the transmission spectra obtained in KBr pellets. The carboxylic group bands are observed at 1610 cm^{-1} and 1410 cm^{-1}(4).

The Fe_2O_3 was floated with glycine as collector at pH 2.7 and 10. The pH was adjusted with HCl and NaOH. The concentrates were heated at 150°F for 12 hours and the ATR spectra recorded. The spectra of Fe_2O_3 floated at pH 2.7 do not show any evidences of adsorbed glycine, and it is speculated that the adsorption, if any, was probably physical and the adsorbed glycine was removed during the drying period. The spectra of Fe_2O_3 floated at pH 10, show the adsorption of glycine. However, the carboxylic bands are slightly shifted and appear at 1630 cm^{-1} and 1390 cm^{-1}.

Adsorption of Oleic Acid: The adsorption of oleic acid on hematite (from Negauree, Mich. obtained from Wards Natural Science Establishment, Inc.) is under investigation. The hematite is floated with oleic acid, the concentrate filtered and dried at 150°F for 12 hours. So far flotation at pH 11 has been carried out. Flotation experiments at other pH values are in progress. The results so far are in accord with the findings of Peck et al.(1).

Discussion

The loss of hydrogen from -COOH groups makes the carbon-oxygen bonds equivalent and consequently two modes, symmetric and antisymmetric stretching are observed(2a). The bands of OH deformation and COH bending disappear. When the carboxylic group is attached

to a metal ion, the symmetric and antisymmetric stretching of C-O are affected. The C-O stretching frequencies observed in this work, and some from other observers are shown in Table II. In acids the antisymmetric stretching corresponds to C = O stretching and the symmetric stretching to C-O.

Table II. Comparison of C-O Stretching Carboxyl Group in Various Systems

System	Antisymmetric Stretching	Symmetric Stretching	Reference
Acetic acid vapor at 150° (monomers)	1799	1279	(3)
Glacial Acetic acid (dimers)	1750	1280	This Work and (2)
Acetate ion (aqueous)	1556	1413	(4a)
Na Acetate	1578	1414	(4a)
Acetic Acid adsorbed on Fe_2O_3	1580	1420	This Work
Glycine solid	1610	1413	This Work and (4)
Glycine adsorbed on Fe_2O_3	1630	1390	This Work
Glycino-Platinum complexes	1640	1380	5

The surface of oxides such as Fe_2O_3 is usually covered with OH groups[6], and these surface OH groups require heating to about 1200°F for their removal. Therefore, under the conditions of our study, it is likely that the bonding of the carboxylic group to the surface of Fe_2O_3 would be through these surface OH groups, and the symmetric and antisymmetric stretching of C-O would be close to those of acetic acid dimers. However, since the observed frequencies are close to those observed in Na-acetate, it seems that the surface Fe^{+++} is bonded directly to COO^- groups. The similarity in the spectra of adsorbed glycine and glycino complexes of platinum further strengthens the conclusion that surface Fe^{+++} are bonded to the oxygens of the carboxylic groups. This bonding is probably electrostatic, and preserves, to some extent, the equivalence of carbon-oxygen bonds of the carboxylic group.

References

1. Peck, A. S., Raby, L. H., and Wadsworth, M. E., Trans. Soc. Min. Eng.
2. Colthup, N. B., Daly, L. H., and Wiberley, S. E., Sept. 1966, p. 301, Introduction to Infrared and Raman Spectroscopy, Academic Press 1964, p. 259, 2a, p. 262.
3. Wilmhurst, J. K., J. Chem. Phys. 25, 1171 (1956).
4. Nakamoto, K., Infrared Spectra of Inorganic and Coordination Compounds, Wiley-Interscience 1970, p. 233, 4a p. 223.

5. Saraceno, A. J., Nakagawa, I., Mizushima, S., Columba, C., and Quagliano, J. V., Bull. Chem. Soc. Japan, 80, 5018 (1958).

6. Parks, G. A., Chem. Rev. 65, 177 (1965).

The Correlation Between Ni and Mg Dissolution from Chrysotile*

by: Merrill Allen

Experimental

Sample preparation and experimental proceedures for the dissolution studies described here are the same as previously noted (1). The dissolution studies were carried out in 1 N HCl and in 1 N HAc. Determinations for Mg and Ni were done by atomic absorbtion spectrophotometry employing a Perkin Elmer model 303 operated using optimum instrumental settings and using an air acetylene flame.

Results

Figure 1 shows graphically the data from the studies. The straight continuous lines show the correlation between Mg and Ni concentrations in the acid solutions. A dashed line is drawn at an "average" position between the curves for the two different acids. Only two points were available from the HAc study as Ni was undetected in the second and third extractions of this study. The constant ratio between the Mg and Ni present in the acid leach solutions indicates that the ratio of dissolution rates of Mg and Ni is constant although the dissolution rates of the two cations are not equal. The fact that the dissolution ratio of Mg and Ni is constant but that the rates of dissolution for the two cations are different indicates that the Ni may be present in two phases, i.e. in chrysotile and in the associated magnetite. At any rate, the correlation between Mg and Ni dissolution allows one to predict the amount of nickel removed from chrysotile by knowing the amount of Mg removed (see Figure 2.).

References

(1) Allen, M. A., "Dissolution and Cation Exchange Properties of Some Asbestos Minerals", Minerals Research Progress Report #1, Dept. of Chem. & Met. Engr., Univ. of Nevada (1971).

* This research was supported by Department of Health, Education and Welfare Research Grant EC00381.

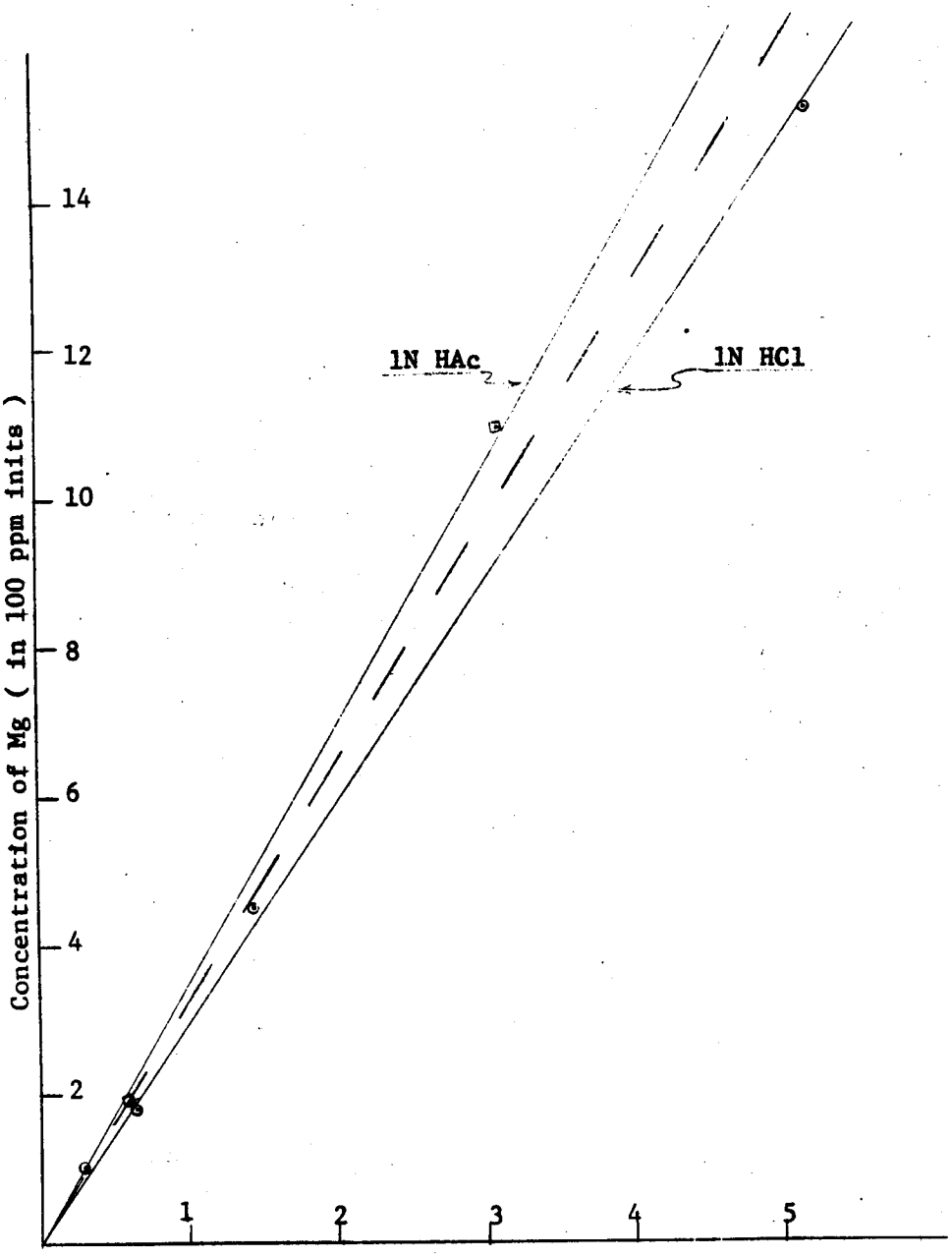

Figure 1. Plot of Ni vs Mg concentration in hydrochloric and acetic acid lelutions used to leach chrysotile.

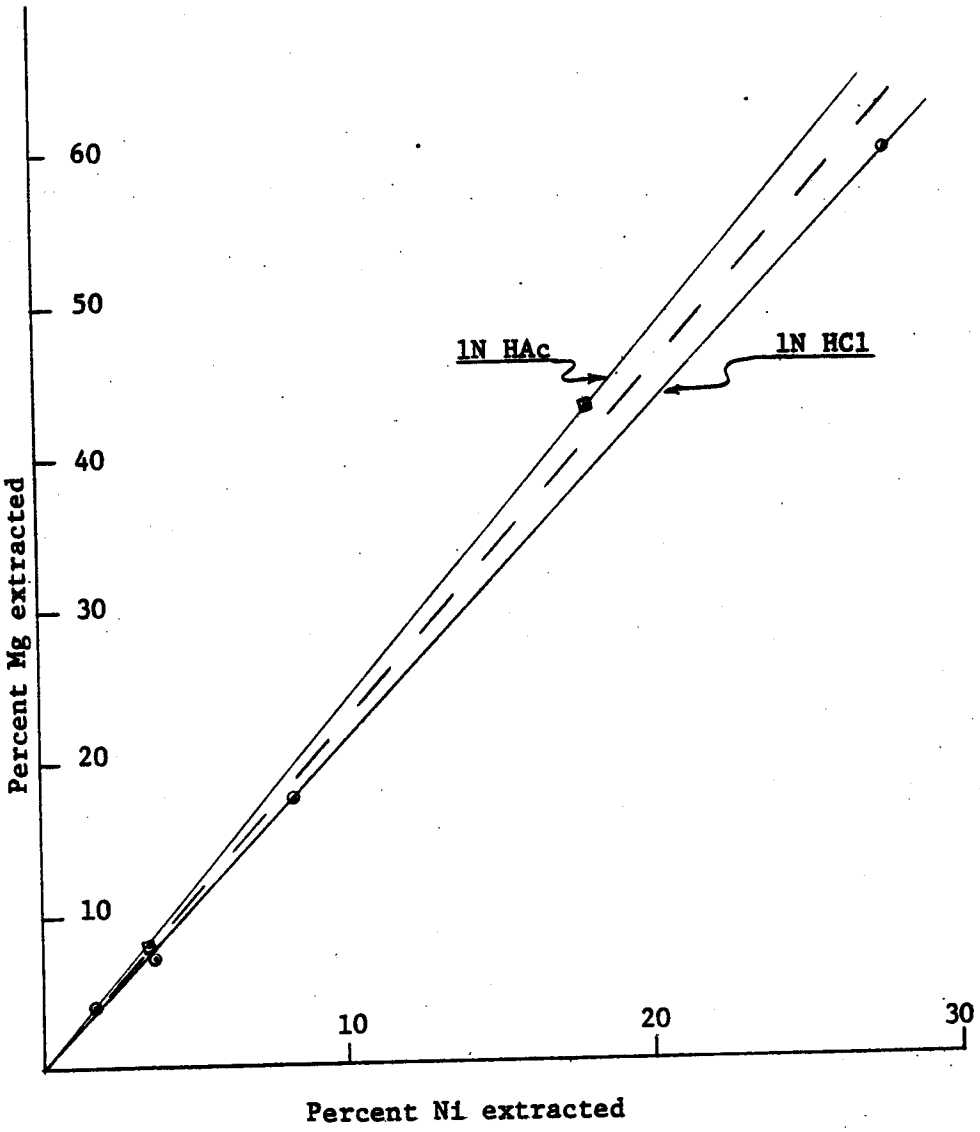

Figure 2. Plot of Ni vs Mg extracted from chrysotile using hydrochloric and acetic acids.

Migration of Asbestos Fibers in the Lymphatic System of Mice*

by: James E. McGuire and Robert E. Thomas
Department of Biological Sciences, California State University, Chico

Mesothelioma of the pleura comparable to that resulting from asbestos exposure in man can easily be induced in the rat and hamster by intrapleural administration of asbestos[1-5]. Induction of pleural and peritoneal mesotheliomata following subcutaneous injection of asbestos into the flank of mice has also been reported[6]. It was suggested that asbestos fibers might migrate from the injection site, in a somewhat selective manner, to the subserosal layer of the thoracic and abdominal viscera. The lymphatic system was suggested as a possible avenue for dissemination. The present study was designed to examine the movement of asbestos fibers through the lymphatic system from a subcutaneous injection site in mice.

Materials and Methods

The asbestos used in this study was a sample of amosite supplied by Dr. Ross Smith (Mackay School of Mines, University of Nevada, Reno). The distributions of fiber lengths were determined by phase contrast microscopy. Sixty-five and one half percent of the fibers were less than five microns in length, 32% were between 5 and 10 μ, and 2.5% were in excess of 10 μ in length. The fibers were suspended in physiological saline before injection.

Swiss Webster mice obtained from a commercial dealer were used in the study. They were housed 5 to 8 per cage and fed standard laboratory chow and water *ad libitum*. Eighty randomly selected mice were injected subcutaneously in the right flank area with 10 mg of amosite suspended in 0.3 ml of physiological saline.

Two mice from the experimental group were sacrificed each day for the first 7 days post injection. One experimental mouse was sacrificed each day for 6 days of the week from the 2nd to the 12th week. Three control animals were sacrificed during the first week and then one control animal per week during the 2nd to the 12th week.

The animals were sacrificed by anesthesia and lymph nodes removed from the right and left inguinal, right and left axillary and mediastinal areas of each animal. A blood sample was obtained from each animal by cardiac puncture. Tissue samples were removed from the injection site of randomly selected animals. Five micron paraffin sections were prepared and the serial sections stained with hematoxylin and eosin.

Results and Discussion

Several techniques were used in an attempt to detect asbestos fibers in tissues including the flurochrome method of Berkley *et al*[7], polarized light microscopy, Perl's staining for iron and light microscopy, and lightly stained hematoxylin and eosin sections. We found that light hematoxylin and eosin staining and phase contrast microscopy was the most reliable method for screening tissue for asbestos fibers. At the present time, complete screening of all lymph nodes removed from 61% of the animals has been completed. Screening of the lymph nodes closest to the injection site has been completed for all animals.

* This research is supported in part by Department of Health, Education and Welfare research grant EC00381.

Asbestos fibers were first noted in the asbestos nodes the second day post injection. This agrees with the results of Kanazawa et al[8] who found asbestos fibers in axillary lymph nodes two days after subcutaneous injection in the flank area. The greatest concentration of fibers in the lymphatics seems to occur at approximately 45 days post injection and the number of intracellular fibers compared to free fibers increases with time after injection. The greatest concentrations of asbestos fibers were found in the ipsilateral inguinal lymph nodes with the next highest concentration in the ipsilateral axillary nodes (Table I). The blood samples which were taken were macerated with heating in 30% KOH. Preliminary results reveal significant concentrations of asbestos fibers in these samples.

Preliminary results are in very close agreement with published results[6,8]. It has been confirmed that asbestos fibers, injected subcutaneously into mice, do spread to other sites and that they are distributed mainly via the lymphatic system. As expected, the proximal lymphatic tissues contain significantly more asbestos than the distal lymphoid tissues.

Table I. Concentration of Asbestos Fibers in Lymphatic Tissues

Lymph Node	Concentration of fibers*
Inguinal (Ipsilateral)	1.00
Inguinal (Contralateral)	0.06
Axillary (Ipsilateral)	0.27
Axillary (Contralateral)	0.31
Mediastinal	0.16

References

1. Wagner, J. C. and G. Berry. 1969. Mesotheliomas in rats following inoculation with asbestos. Brit. J. Cancer. 23:567-581.

2. _____. 1962. Experimental production of mesothelial tumors of the pleura by implantation of dusts in laboratory animals. Nature (London) 196:180-181.

3. _____, G. Berry, and V. Timbrell. 1970. Mesotheliomas in rats following the intrapleural inoculation of asbestos. In Pneumoconiosis: Proceedings of the International Conference. Johannesburg, 1969. (H.A. Shapiro, ed.) New York, Oxford University Press, pp. 216.

4. Stanton, M. F., R. Blackwell, and E. Miller. 1969. Experimental pulmonary carcinogenesis with asbestos. Amer. Industr. Hyg. Assoc. J. 30:236-244.

5. _____, and Constance Wrench. 1972. Mechanisms of mesothelioma induction with asbestos and fibrous glass. J. Nat. Can. Inst. 48:797-821.

6. Roe, F. J. C., R. L. Carter, M. A. Walters, and J. S. Harington. 1967. The pathological effects of subcutaneous injections of asbestos fibers in mice: Migration of fibers to submesothelial tissues and induction of mesotheliomata. Int. J. Cancer. 2:628-638

* Concentration of fibers in the different lymph nodes was compared by assigning a rank value of one to the ipsilateral inguinal node.

7. Berkley, C., J. Churg, I. Selikoff, and W. E. Smith. 1965. The detection and localization of mineral fibers in tissue. Ann. N. Y. Acad. Sci. 132:48-63.

8. Kanazawa, K., M. S. C. Birbeck, R. L. Carter, and F. J. C. Roe. 1970. Migration of asbestos fibers from subcutaneous injection sites in mice. Brit. J. Can. 24:96-106.

Carcinogenesis of Asbestos Fibers as Related to Surface Chemistry*

by: Robert E. Thomas
Department of Biological Sciences, California State University, Chico

Mesothelioma of the pleura comparable to that resulting from asbestos exposure in man can be easily induced in the rat and hamster by intrapleural administration of asbestos[1-6]. Experiments of this type readily indicate the carcinogenicity of asbestos and afford an excellent means of investigating the carcinogenic mechanisms involved.

The shape, surface area and other physical factors of the asbestos fibers have been suggested as contributing to the carcinogenic nature of these minerals[7-10]. The purpose of this study was to investigate the relationship between the surface chemistry of the fibers and their carcinogenicity.

Materials and Methods

Two hundred and forty Wistar strain rats purchased from a commercial dealer were used in these studies. The rats were housed 2 to 5 per cage and fed standard laboratory chow and water ad libitum. Test materials were injected into the thoracic cavity of rats when they were between 10 and 15 weeks of age. The asbestos samples were prepared at the Mackay School of Mines, University of Nevada by cutting with a modified Waring blender for 90 to 120 minutes and included the following: chrysotile A from Quebec, chrysotile B from California, amosite, and crocidolite. In an attempt to alter the surface characteristics of the fibers, samples of each type fiber were treated as follows: leaching in 1N HCl for one hour, aging in distilled water for one week, and aging in distilled water for six months. Additional samples were prepared by cutting and passing through 325 mesh screens. Samples of each type of fiber prepared by this procedure were leached in 6N HCl for two hours. In addition to the asbestos fibers prepared by this method, untreated and acid treated serpentine samples were also prepared. The asbestos samples were suspended in physiological saline to give a final concentration of 50 mg/ml. One half ml of the solution was injected intrapleural via an 18 gauge needle. Control animals were injected similarly with 0.5 ml of sterile physiological saline.

All groups were observed daily. After six months one rat was sacrificed per month from one of the untreated asbestos sample groups until the first death attributed to mesothelioma was noted at 12 months. The weight of each rat was recorded weekly and after the 12th month only moribund rats were killed. Intrapleural neoplasms were detected only at necropsy. Animals surviving are being killed during the 25th month post injection and detailed gross necropsy is being performed on each animal. Five to ten micron paraffin sections of selected neoplasms are stained with hematoxylin and eosin, Van Gieson and hematoxylin, Perl's and saffanin, and Periodic Acid Schiffs.

Results and Discussion

The number of animals receiving each treatment and surviving after 30 days can be seen in Table I. The few animals which died within 30 days of treatment were considered to have died as a result of the injection or subsequent infection. In all cases these animals were not considered in the analysis of the results but were replaced with other animals where possible.

*This research is supported by Department of Health, Education and Welfare research grant EC00381.

Table I. Numbers of Experimental Animals

Sample	Number of Animals	Necropsies Performed to Date
Chrysotile A (Untreated)	8	8
" (1 N HCl-1 hr)	8	8
" (H_2O-1 wk)	8	2
" (H_2O-6 mo)	8	0
Chrysotile B (Untreated)	8	8
" (1N HCl-1 hr)	8	8
" (H_2O-1 wk)	8	2
" (H_2O-6 mo)	8	0
Amosite (Untreated)	8	8
" (1N HCl-1 hr)	8	8
" (H_2O-1 wk)	8	4
" (H_2O-6 mo)	8	0
Crocidolite (Untreated)	8	8
" (1N HCl-1 hr)	8	8
" (H_2O-1 wk)	8	4
" (H_2O-6 mo)	8	0
Chrysotile A-325 (Untreated)	8	0
" " (6N HCl-2 hr)	8	0
Chrysotile B-325 (Untreated)	8	8
" " (6N HCl-2 hr)	8	4
Amosite 325 (Untreated)	8	0
" " (6N HCl-2 hr)	8	0
Crocidolite 325 (Untreated)	8	4
" " (6N HCl-2hr)	8	0
Serpentine 325 (Untreated)	8	2
" " (6N HCl-2 hr)	8	4
Saline Controls	16	8
Mg 0	8	2
Fe_2O_3	8	2

Table II lists the results of the post-mortem examination. Fifty-four per cent of the animals receiving an injection of asbestos developed mesothelioma. The first death resulting from a mesothelioma occurred in the crocidolite group 54 weeks after injection. Two further lethal mesotheliomas were noted in this group at 66 and 76 weeks. Lethal mesotheliomas occurred in the chrysotile group at 65, 65, 70 and 72 weeks post injection. The first lethal mesotheliomas in the amosite animals did not occur until the 81st week. This does not agree with the results obtained by Stanton[9] and Wagner[1,11] who found an earlier occurrence of mesothelioma with amosite than with chrysotile or crocidolite. It should be pointed out, however, that at this point of the study, 80 per cent of the posted animals which received amosite have developed mesothelioma compared to only 40 per cent and 54 per cent for chrysotile and crocidolite respectively.

Fibrosis within the thoracic cavity was evident in all the animals receiving asbestos injections with but two exceptions. It is expected that the injections were somehow misplaced in these two instances. Neoplasms outside the pleural cavity were found in approximately 19 per cent of the animals posted to date. Mammary neoplasms have been found in approximately 21 per cent of our animals. In most instances the mammary tumors were surgically removed and histologic examination performed. Other common neoplasms noted involved the adrenals and genital organs.

The animals which developed mesotheliomas appeared to be under no physical stress until just before death. In the majority of these animals, death appeared to be due to a large intrapleural hemorrhage. The tumors found varied in size from a large mass completely enveloping the right lung to a few small nodules on the parietal pleura and diaphram. Histologically, the tumors appear to be similar to those reported in other studies with spindle cells predominating[1,5,10].

At this point of the study, no statistical analysis would be valid and no conclusions can be made regarding the effect of the acid and water leaching of the asbestos fibers on carcinogenesis. Indications are, however that there will be no appreciable differences. The relationship between fiber size and tumor yield also awaits analysis.

Table II. Necropsy Findings

Sample	Number of animals	Mesothelioma	Other Neoplasms	Fibrosis
Chrysotile A (Untreated)	8	4	2	8
" (1N HCl-1 hr)	8	4	1	7
" (H_2O-1 wk)	2	1	1	2
" (H_2O-6 mo)	0			
Chrysotile B (Untreated)	8	6	3	8
" (1N HCl-1 hr)	8	6	3	8
" (H_2O-1 wk)	2	0	1	2
" (H_2O-1 mo)	0			
Amosite (Untreated)	8	4	1	8
" (1N HCl-1 hr)	8	8	1	8
" (H_2O-1 wk)	4	4	0	4
" (H_2O-6 mo	0			
Crocidolite (Untreated)	8	4	2	8
" (1N HCl-1 hr)	8	4	1	8
" (H_2O-1 wk)	4	2	0	4
" (H_2O-6 mo)	0			
Chrysotile A-325 (Untreated)	0			
" " (6N HCl-2 hr)	0			
Chrysotile B-325 (Untreated)	8	4	1	8
" " (6N HCl-2 hr)	4	0	0	4
Amosite 325 (Untreated)	0			
" " (6N HCl-2 hr)	0			
Crocidolite 325 (Untreated)	4	3		4
" " (6N HCl-2 hr)	0			
Serpentine 325 (Untreated)	2	0	1	2
" " (6N HCl-2 hr)	4	0	1	4
Saline Controls	8	0	3	0
Mg 0	2	0	3	0
Fe_2O_3	2	0	0	1

References

1. Wagner, J. C. and G. Berry. 1969. Mesotheliomas in rats following inoculation with asbestos. Brit. J. Cancer. 23:567-581.

2. _____. 1962. Experimental production of mesothelial tumors of the pleura by implantation of dusts in laboratory animals. Nature (London) 196:180-181.

3. _____, G. Berry, and V. Timbrell. 1970. Mesotheliomas in rats following the intrapleural inoculation of asbestos. In Pneumociosis: Proceedings of the International Conference. Johannesburg, 1969. (H.A. Shapiro, ed.) New York, Oxford University Press. pp. 216.

4. Stanton, M. F., R. Blackwell, and E. Miller. 1969. Experimental pulmonary carcinogenesis with asbestos. Amer. Industr. Hyg. Assoc. J. 30:236-244.

5. _____, and Constance Wrench. 1972. Mechanisms of mesothelioma induction with asbestos and fibrous glass. J. Nat. Can. Inst. 48:797-821.

6. Donna, A. 1970. Tumori sperimentali da amianto di crisotile, crocidolite e amosite in ratto Sprague-Dawley. Med. Lavor. 61:1-32.

7. Harington, J. S., F. C. Roe, and M. Walters. 1967. Studies of the mode of action of asbestos as a carcinogen. S. Afri. Med. J. 41-800.

8. Kogan, F. M., S. Troitskii, and N. N. Vdilova. 1966. Data on mechanisms of fibrogenic action of asbestos dust. 1966. Abstract in Chem Abstracts 66:27435 v.

9. Bryson, G. and F. Bischoff. 1967. Silicate induced neoplasms. Progr. Exp. Tumor. Res. 9:77-164.

10. Churg, J., S. H. Rosen, and S. Moolten. 1965. Histological characteristics of mesothelioma associated with asbestos. Ann. N. Y. Acad. Sci. 132:614-622.

11. Timbrell, V., D. M. Griffiths, and F. D. Pooley. 1971. Possible biological importance of fibre diameters of South African amphiboles. Nature (London) 232:55-56.